AGU PUBLICATIONS

JGR

Journal of Geophysical Research: Solid Earth

RESEARCH ARTICLE
10.1002/2017JB014150

Key Points:
- High-resolution images of crustal discontinuities beneath the Illinois Basin area reveal strong variations of the crustal thickness
- Anomalously thick crust exists beneath the central and southeastern Illinois Basin area, surrounded by relatively thin crust beneath arches
- Four crustal thickening hypotheses are examined, predating and possibly contributing to the formation and development of the Illinois Basin

Supporting Information:
- Supporting Information S1
- Movie S1
- Movie S2
- Data Set S1
- Data Set S2

Correspondence to:
X. Yang,
xiaotaoyang@umass.edu

Citation:
Yang, X., G. L. Pavlis, M. W. Hamburger, S. Marshak, H. Gilbert, J. Rupp, T. H., Larson, C. Chen, and N. S. Carpenter (2017), Detailed crustal thickness variations beneath the Illinois Basin area: Implications for crustal evolution of the midcontinent, *J. Geophys. Res. Solid Earth*, *122*, 6323–6345, doi:10.1002/2017JB014150.

Received 28 FEB 2017
Accepted 11 JUL 2017
Accepted article online 12 JUL 2017
Published online 1 AUG 2017

Detailed crustal thickness variations beneath the Illinois Basin area: Implications for crustal evolution of the midcontinent

Xiaotao Yang[1,2], Gary L. Pavlis[1], Michael W. Hamburger[1], Stephen Marshak[3], Hersh Gilbert[4,5], John Rupp[6], Timothy H. Larson[7], Chen Chen[4], and N. Seth Carpenter[8]

[1]Department of Geological Sciences, Indiana University Bloomington, Bloomington, Indiana, USA, [2]Now at Department of Geosciences, University of Massachusetts Amherst, Amherst, Massachusetts, USA, [3]School of Earth, Society, and Environment, University of Illinois at Urbana-Champaign, Urbana, Illinois, USA, [4]Department of Earth, Atmospheric, and Planetary Sciences, Purdue University, West Lafayette, Indiana, USA, [5]Now at Department of Geoscience, University of Calgary, Calgary, Alberta, Canada, [6]Indiana Geological Survey, Indiana University Bloomington, Bloomington, Indiana, USA, [7]Illinois State Geological Survey, Champaign, Illinois, USA, [8]Kentucky Geological Survey, University of Kentucky, Lexington, Kentucky, USA

Abstract We present high-resolution imaging results of crustal and upper mantle velocity discontinuities across the Illinois Basin area using both common conversion point stacking and plane wave migration methods applied to *P* wave receiver functions from the EarthScope Ozark, Illinois, Indiana, and Kentucky experiment. The images reveal unusually thick crust (up to 62 km) throughout the central and southeastern Illinois Basin area. A significant Moho gradient underlies the NW trending Ste. Genevieve Fault Zone, which delineates the boundary between the Illinois Basin and Ozark Dome. Relatively thinner crust (<45 km) underlies most of the Precambrian highlands surrounding the Illinois Basin and beneath the rift-related structures of the Reelfoot Rift and the Rough Creek Graben. We consider four hypotheses to explain the presence of thick crust under the central and southeastern Illinois Basin. Crustal thickening may have been produced (1) prior to its accretion to North America around 1.55 Ga and is an inherited characteristic of this crustal province; (2) by underthrusting or shortening during Proterozoic convergent margin tectonics around 1.55–1.35 Ga; (3) by Late Precambrian magmatic underplating at the base of older crust, associated with the creation of the Eastern Granite-Rhyolite Province around 1.3 Ga; and (4) through crustal "relamination" during an episode of Proterozoic flat-slab subduction beneath the Illinois Basin, possibly associated with the Grenville Orogeny.

1. Introduction

The North American craton is the portion of the North American continent that has not undergone penetrative deformation and metamorphism since the end of the Latest Precambrian to Early Cambrian rifting events. This craton includes the Canadian Shield, where broad areas of Precambrian igneous and metamorphic rocks are exposed at the Earth's surface, and the cratonic platform, on which a cover of minimally deformed Phanerozoic sedimentary strata overlies the Precambrian basement complex. This complex is composed of Archean lithosphere blocks that were sutured to each other during Paleoproterozoic collisional orogenies, as well as broad Yavapai (1.8 to 1.7 Ga) and Mazatzal (1.65 to 1.6 Ga) provinces that were accreted onto the southeastern margin of the continent [*Hoffman*, 1988; *Whitmeyer and Karlstrom*, 2007] (Figure 1 and Table 1). A large part of the area underlain by these orogenic belts was affected by a 1.55 to 1.35 Ga interval of felsic intrusion and extrusion, which yielded the Eastern Granite-Rhyolite Province (EGRP). The poorly known Picuris Orogeny (1.55 to 1.35 Ga) may also have deformed and/or added crust to this region [*Daniel et al.*, 2013]. A distinct NE trending boundary, known as the Nd-line, separates crust containing pre-1.6 Ga juvenile components to the northwest, from crust containing post-1.6 Ga juvenile components to the southeast [*Bickford et al.*, 2015, 1986]. At about 1.1 Ga, the Grenville Orogeny, a major continental collision, resulted in the accretion of additional lithospheric material onto the eastern and southern parts of the continent. At various times during the Late Proterozoic, thick accumulations of sediments and/or volcanics spread across portions of the craton. Additionally, localized rifting events produced basement penetrating faults, allowing for the preservation of sediments and volcanics in narrow troughs. The largest of these, the Midcontinent Rift, has a length of over 1300 km [*Stein et al.*, 2016].

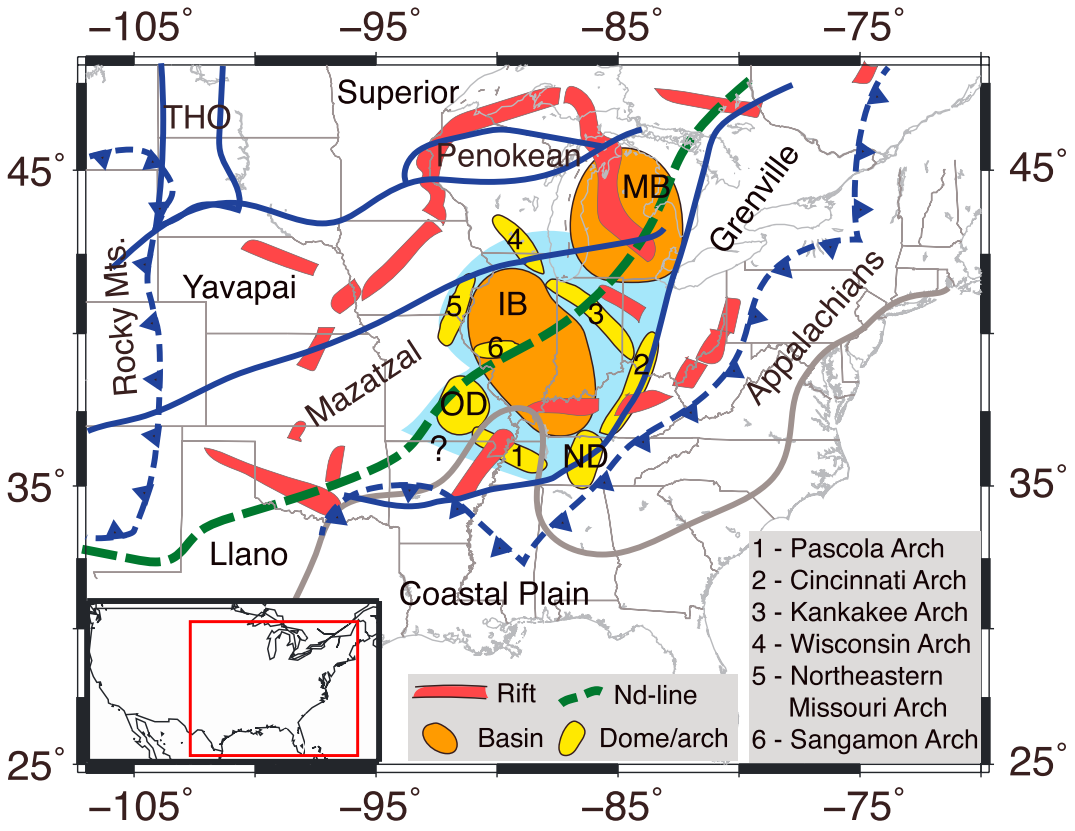

Figure 1. Physiographic provinces of the central and eastern United States highlighting the major structural units in our study area centering on the Illinois Basin. Span of the tectonic provinces are based on *Marshak et al.* [2017]. Locations of the domes and arches surrounding the Illinois Basin are plotted after *Nelson and Marshak* [1996]. Outline of the Illinois Basin is modified after *Buschbach and Kolata* [1999]. The Eastern Granite-Rhyolite Province is shown as shaded light blue area after *Bickford et al.* [2015]. THO = Trans-Hudson Orogeny, OD = Ozark Dome, ND = Nashville Dome, IB = Illinois Basin, MB = Michigan Basin.

The North American craton, however, has not acted like a fully rigid block in the Phanerozoic. It underwent notable deformation during the Late Neoproterozoic and through the Phanerozoic in the form of regional-scale intracratonic basins, domes, and arches, as well as by displacements in local fault-and-fold zones [*Marshak and Paulsen*, 1996, 1997; *McBride and Nelson*, 1999]. Some fold-and-fault zones of the cratonic platform remain active today, as manifested by contemporary Midcontinent seismicity [*Stein and Liu*, 2009]. Evolution of cratonic basins, such as the Illinois, Michigan, and Williston Basins, has been linked with larger-scale rifting and other orogenic events [*Heidlauf et al.*, 1986; *Klein and Hsui*, 1987a, 1987b]. This paper provides new results focusing on the deep crustal structure of the Illinois Basin and surrounding area that

Table 1. Timeline of Major Tectonic Events in the Central and Eastern North American Continent From Meso-Proterozoic to Paleozoic Eras Extracted After *Whitmeyer and Karlstrom* [2007] and *Hatcher* [2010]

Time Frame (Ga)	Major Events	Major Resultant Structures
1.65–1.6	Development of Mazatzal Orogeny	Mazatzal Province
1.55–1.35	Meso-Proterozoic tectonic events including magmatism, metamorphism, and deformation (e.g., Picuris Orogeny)	Granite-Rhyolite Province, Nd-line
1.3–1.09	Grenville tectonism (final assembly of Rodinia): intracratonic extension and voluminous mafic magmatism	Eastern Granite-Rhyolite Province, Grenville Province, Midcontinent Rift
0.78–0.68	Early breakup of Rodinia at its west coast	Western breakup rifts
0.62–0.55	Main phase of Rodinia breakup along its eastern margin	Rome Trough
0.55–0.535	Final phase breakup of Rodinia with detachment of the Argentine Precordillera: formation of the midcontinent failed rift arms	Reelfoot Rift, Oklahoma Aulacogen
0.49–0.26	Appalachian orogenic events	Appalachians

offer insights on the assembly of the North America Midcontinent during the Late Proterozoic Era and possible constraints on present-day reactivation of these inherited structures.

The Illinois Basin is defined as a NNW trending elliptical depression covering about 155,000 km^2 in parts of Illinois, Indiana, and Kentucky [*Buschbach and Kolata*, 1991] (Figures 1 and 2). The basement beneath the Illinois Basin consists of rocks of the EGRP that presumably overlie older crust accreted during the Mazatzal and/or Picuris orogenies (Figure 1 and Table 1) [*Bickford et al*., 2015; *Whitmeyer and Karlstrom*, 2007]. The Nd-line, as the boundary separating the Mazatzal Province to the northwest to the younger juvenile crust to the southeast, referred to as post-Mazatzal terrane for easy description, cuts diagonally across the central part of the basin (Figure 1). Neoproterozoic stratified rocks locally overlie portions of the Granite-Rhyolite basement, but their distribution has not been extensively documented or sampled [*Baranoski et al*., 2009; *Drahovzal et al*., 1992]. Most of the basin fill consists of Cambrian through Pennsylvanian strata deposited as the basin subsided, in pulses, during the Paleozoic. Initially, the basin was open to the south, but growth of the NW trending Pascola Arch at the end of the Paleozoic uplifted the southern boundary of the basin, separating the Illinois Basin from the Mississippi Embayment to the south. The basin is bounded on the southwest by the Ozark Dome, on the west by the Northeastern Missouri Arch, on the northeast by the Kankakee Arch, and on the east by the Cincinnati Arch (Figure 1). The depth to the Precambrian basement in this area varies dramatically [*Domrois et al*., 2015; *Marshak et al*., 2017].

For decades, researchers have worked to characterize the deep structure beneath this intracratonic basin and to improve understanding of adjoining arches and domes. Active source seismic surveys have outlined first-order structures of the Precambrian basement [*Pratt et al*., 1989, 1992] and some of the Paleozoic sequences [*Duchek et al*., 2004; *McBride et al*., 2003, 2007; *McBride and Nelson*, 1999; *Okure and McBride*, 2006] in the southern Illinois Basin. *Hildenbrand et al.* [1996] investigated the northwest trending Missouri gravity low (Figure S1a in the supporting information) and proposed the existence of a series of thick, low-density batholiths in the underlying crust, which may be the manifestations of a mantle plume during Late Precambrian time that heated the crust. *McBride et al.* [2003] observed seismic reflectors overlying the Proterozoic EGRP below the Paleozoic cover in the central-eastern Illinois. They interpreted these reflector sequences as the remnants of a Proterozoic rhyolitic caldera complex and/or rift episode related to the original thermal event that produced the Granite-Rhyolite Province. *Bedle and van der Lee* [2006] imaged the upper mantle structure using surface waves from local earthquakes recorded by regional seismic stations. They proposed a fossilized flat-slab subduction in the uppermost mantle below about 90 km beneath the Illinois Basin. Shear velocities have revealed heterogeneities beneath the Illinois Basin area [*Chen et al*., 2016; *Chu and Helmberger*, 2014; *Pollitz and Mooney*, 2016]. *Shen and Ritzwoller* [2016] and *McGlannan and Gilbert* [2016] all observed relatively thick crust in the broad southern Illinois Basin area. In addition, wide-angle seismic reflection and refraction studies have imaged a high-velocity layer at the bottom of the crust in the Reelfoot Rift region [*Nelson and Zhang*, 1991], interpreted as evidence of lower crust magmatic underplating that may be associated with the rifting process. These studies have provided useful information on primary crustal velocity structure beneath the midcontinent in our study area. This paper adds to that body of knowledge by revealing previously unknown, higher-resolution details of the geometry of the crust-mantle boundary.

The present-day structural relief of the basin is manifested by the configuration of the contact between Precambrian basement and overlying Phanerozoic strata (the Great Unconformity). This contact lies at an elevation of up to 500 m above sea level in the Ozark Dome region, but at a depth of $>$7 km in the Rough Creek Graben region at the southeastern end of the basin [*Bayley et al*., 1968; *Domrois et al*., 2015; *Marshak et al*., 2017]. Thus, there is more than 7.5 km of relief on this surface between the deepest point in the Illinois Basin and the highest point on the adjoining Ozark Dome (Figure 2). The Ste. Genevieve Fault Zone (SGFZ), a major northwest trending fault system located in southwestern Illinois and eastern Missouri [*Marshak and Paulsen*, 1996, 1997; *Nelson*, 1995], forms the southwest boundary of the basin. This fault zone has been mapped for approximately 190 km along strike from the northeastern flank of the Ozark Dome in southeastern Missouri into southwestern Illinois [*Harrison and Schultz*, 2002; *Nelson and Lumm*, 1985]. *Nelson and Lumm* [1985] argue that these faults underwent two major episodes of faulting activity in Late Devonian and in Latest Mississippian through Early Pennsylvanian time. They suggested a mechanism of vertical upthrusting of the basement for the Carboniferous faulting with a nearly vertical master fault at depth

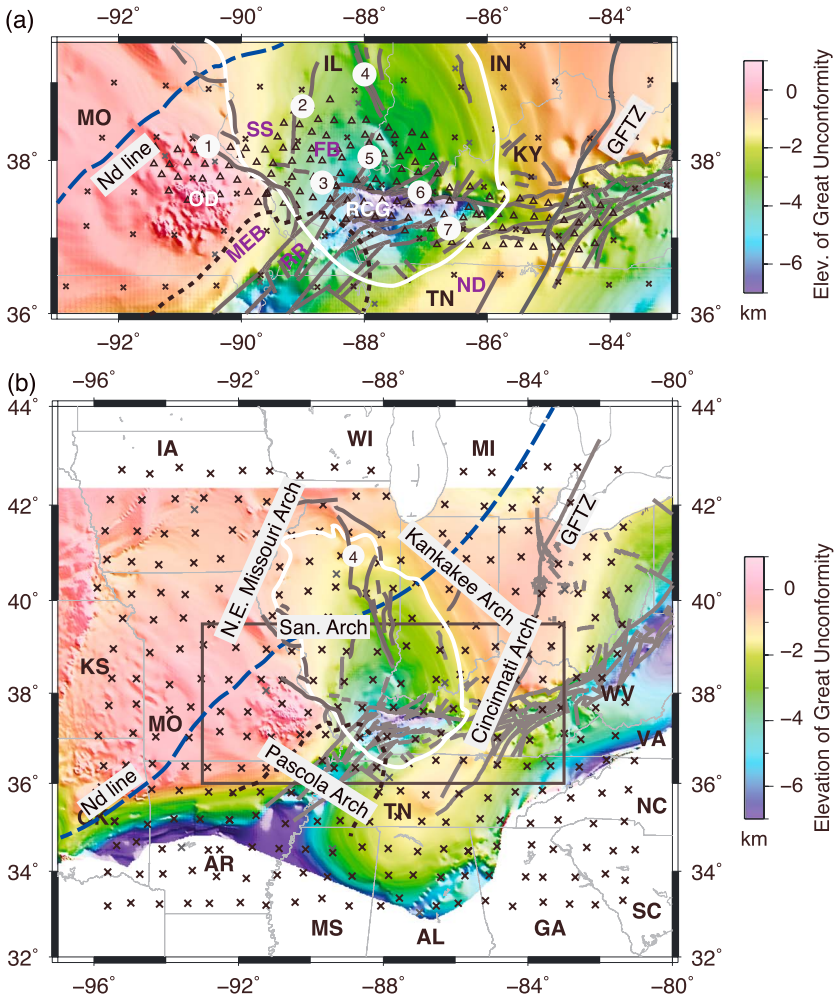

Figure 2. Map of study area showing location of seismic stations. (a) OIINK study area and (b) the CUS regional control area. The solid box in Figure 2b outlines the OIINK study area as mapped in Figure 2a. OIINK flexible array stations are shown as triangles, while stations from other regional seismic networks are shown as crosses. Elevation data of the Great Unconformity is from *Domrois et al.* [2015] and *Marshak et al.* [2017]. This same surface is displayed in a 3-D visualization in Movies S1 and S2. Fault trace data are from *Hickman* [2011]. Outline of the Illinois Basin is shown as thick white line after *Buschbach and Kolata* [1991], defined as the −500 feet contour on top of the Ottawa Supergroup through southern Illinois, Kentucky, and Indiana and the erosional edge of Pennsylvanian strata in northern and western Illinois [*Buschbach and Kolata*, 1991]. 1 = Ste. Genevieve Fault Zone (SGFZ), 2 = Du Quoin Monocline (DQM), 3 = Cottage Grove Fault System (CGFS), 4 = La Salle Anticlinal Belt (LSAB), 5 = Wabash Valley Fault System (WVFS), 6 = Rough Creek-Shawneetown Fault System, 7 = Pennyrile Fault. Abbreviations of structures: MEB = Mississippi Embayment (outlined by the thin dashed line), SS = Sparta Shelf, FB = Fairfield Basin, GFTZ = Grenville Front Tectonic Zone, San. Arch = Sangamon Arch.

penetrating the entire crust. Although there is no evidence that Quaternary strata have been displaced, *Yang et al.* [2014], with the Ozark, Illinois, Indiana, and Kentucky (OIINK) array data, have documented small earthquakes in the regions around this fault zone, with elevated seismicity levels relative to the surrounding area. However, the lack of information about the deep structure beneath this fault zone has limited our understanding of the formation and evolution of the SGFZ and its relationship with the evolution of the Illinois Basin.

It has long been recognized that the Rough Creek Graben is intimately linked to the Reelfoot Rift [*Braile et al.*, 1982a, 1986, 1982b; *Hildenbrand and Hendricks*, 1995; *Liang and Langston*, 2009]. *Braile et al.* [1982a, 1982b, 1986] used seismicity, seismic reflection profiles, and potential field data to argue for the existence of a three-armed rift structure linked to the Reelfoot Rift. They labeled the two other arms, besides the well-defined Rough Creek Graben, as the "St. Louis Arm" and the "Indiana Arm." The proposed St. Louis Arm

follows the trend of the Mississippi River between Missouri and Illinois, coincident with the SGFZ. The Indiana Arm was extrapolated to underlie the Wabash Valley Fault System in southern Indiana. However, subsequent studies of crustal structures [*Catchings*, 1999; *Pratt et al*., 1989; *René and Stanonis*, 1995] and seismicity have made existence of this three-armed rift structure debatable [*Pavlis et al*., 2002; *Yang et al*., 2014]. This paper addresses this debate through high-resolution images of crustal velocity discontinuities associated with these structures.

This study of the Illinois Basin and the regions around it benefits from the newly available data of the Ozark, Illinois, Indiana, and Kentucky (OIINK) EarthScope Flexible Array experiment [*Chen et al*., 2016; *Yang et al*., 2014]. This paper builds upon a recent study by *McGlannan and Gilbert* [2016] that used *P* wave receiver functions from the EarthScope Transportable Array (TA) to produce a regional map of the crust-mantle boundary similar to the one presented here. We extend their result significantly, however, by using newer and denser data from the OIINK flexible array, combined with a higher-resolution imaging technique, to produce significantly higher-resolution images than feasible with the TA data alone. The primary purpose of this paper is to document the new imaging results from the OIINK experiment in combination with consistently processed TA data. These results provide new insights on the geometry of the crustal velocity discontinuities in this region and, therefore, characterize variations in crustal thickness. These new results have important implications on the tectonic history of the North America Midcontinent in general and the Illinois Basin in particular.

2. Data and Method

2.1. Teleseismic *P* Wave Receiver Functions

Figure 2 shows the locations of the seismic stations that provided data for this study. It illustrates the significant difference in sampling density provided by the OIINK stations (Figure 2a) when compared to the regional-scale coverage provided by other TA stations (Figure 2b). To handle this mixed resolution, we processed these data on two scales. Within the footprint of the OIINK experiment (the map area of Figure 2a), data from OIINK flexible array stations were combined with data from additional regional networks within the larger Central United States (CUS) region. The seismic stations in the OIINK study area includes 143 OIINK stations, 80 TA stations, eight Cooperative New Madrid Seismic Network stations, and three stations from the Global Seismographic Network (GSN). The average station spacing of the OIINK Flexible Array is about 25 km, while the average station spacing of the TA is about 70 km. Other regional stations are irregularly distributed. For the CUS study area (Figure 2b), we used data from 314 stations consisting of 302 USArray TA stations, eight United States National Seismic Network stations, three GSN stations, and one station from the network of Portable Observatories for Lithospheric Analysis and Research Investigating Seismicity. We emphasize that we intentionally did not mix the higher-density data comprising the OIINK image with the regional-scale data for the CUS image. We did this to provide more uniform resolution for the CUS image.

We define events in this study as teleseismic earthquakes with a great circle distance between 30° and 95° from the center of the OIINK flexible array (at 38°N, 88.5°W). The OIINK waveform data are from 3137 teleseismic events that occurred between 1 February 2011 and 26 October 2015 with magnitudes $\geq$5.0 (Figure 3a). We selected waveform segments for processing from computed *P* arrival time based on the IASP91 Earth model [*Kennett and Engdahl*, 1991]. We assembled the CUS waveform data from 4545 earthquakes that occurred between February 2010 and March 2014 (Figure 3d). We utilized only the seismograms with first arrival picks for these earthquakes measured by the USArray Array Network Facility. This data set includes waveforms mainly from events greater than magnitude about 5.0 with workable signals.

We estimated 179,244 and 291,020 three-component *P* wave receiver functions for the OIINK and CUS data sets, respectively. The receiver functions were estimated with the generalized iterative deconvolution method of *Wang and Pavlis* [2016]. All receiver function estimates have lengths of 150 s (30 s before to 120 s after the direct *P* arrival). We filtered the data using Butterworth band-pass filters of 0.2 Hz–5 Hz for OIINK data and 0.02 Hz–5 Hz for CUS data. For the OIINK data, we found that using a higher lower corner frequency (0.2 Hz) improved data quality. Table S1 in the supporting information lists the major parameters used in deconvolution for these two data sets, highlighting the parameters with different values. Text S1 in the supporting information documents details of the preprocessing procedures, including automated

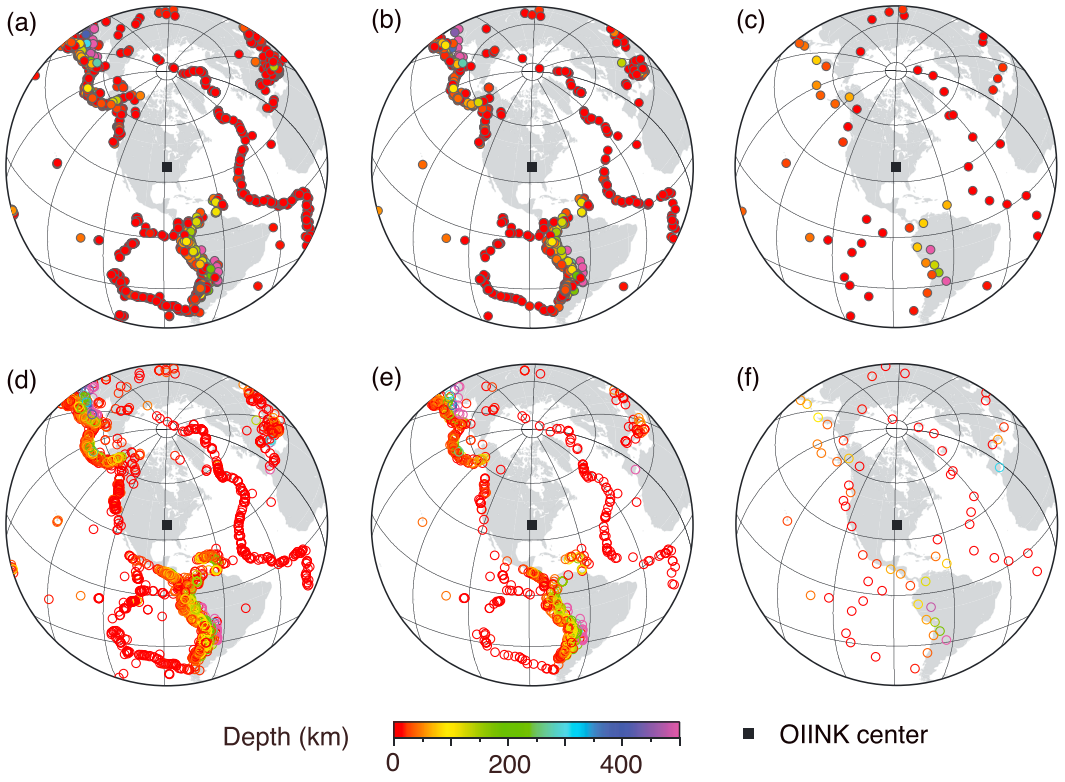

Figure 3. Epicenters of the teleseismic events in (a–c) OIINK data set and in (d–f) CUS data set, colored by source depths. Figures 3a and 3d show the events in the raw data sets, Figures 3b and 3e are the events after removing low-quality data through quality control using the method of *Yang et al.* [2016], and Figures 3c and 3f are the composite earthquakes after applying source-side stacking following *Pavlis* [2011a].

quality control using *RFeditor* by *Yang et al.* [2016] (Figures 3b and 3e), source-side stacking (Figures 3c and 3f), static corrections (Figures S1 and S2), and pseudostation stacking (Figure S3). For static corrections, we built the static model using a 3-D basin-scale sediment thickness model from *Ellett and Naylor* [2016], with constant velocities assigned to each formation (Table S3).

2.2. Migration Imaging

For the OIINK study area, we conducted both plane wave migration (PWMIG) and common conversion point (CCP) stacking for cross-validation. The CCP stacking technique utilized in this study is a special case of the full 3-D PWMIG algorithm by *Pavlis* [2011b] using only the central *P*-to-*S* converted wavefield satisfying Snell's law for seismic ray propagation, instead of the full 3-D scattered wavefield. For brevity, we include only the PWMIG results in this paper for the OIINK region. See *Yang* [2016] for comparison with the CCP stacking results. The PWMIG processing used an 11×11 rectangular slowness grid centered on the incident wave slowness computed by IASP91 [*Kennett and Engdahl*, 1991] from -0.05 s/km to 0.05 s/km with spacing of 0.01 s/km. We applied a top mute operator to the data to remove the incident wavefield, following *Poppeliers and Pavlis* [2003] and *Pavlis* [2011b]. For the CUS study area, we only conducted CCP stacking. The relatively large station spacing of about 70 km compared to the Moho depth creates excessive smoothing with PWMIG that degraded rather than improved the resolution of the results. We used the 3-D shear velocity model for the Central U.S. from *Chen et al.* [2016] as the migration model for both the OIINK and CUS data sets.

3. Results

We manually picked the velocity discontinuities shown in this study using Schlumberger's seismic interpretation package, *Petrel*, with assistance from its automated surface-tracking feature. Figure S4 shows the medians of the fold counts, which we define as the number of composite earthquakes shown in Figures 3c and 3f contributing to the image points, within ±2 km around the Moho surfaces determined from the

imaging results. In general, except for the edges, the median fold counts for all data sets are higher than 15. We emphasize that the total number of seismograms contributing to each cell is, in all cases, significantly higher than this metric because composite earthquakes are stacks of multiple events from the same source region. Movies S1 and S2 in the supporting information show vertical profiles slicing through the image volumes from the OIINK PWMIG (Movie S1 and Data Set S1 in the supporting information for Moho data) and the CUS CCP stacking (Movie S2 and Data Set S2 for Moho data) results. Readers are encouraged to examine these animations to appraise the validity of our interpretations (see Text S2 for details).

3.1. Moho Depth

Depth and amplitude variations of the Moho and other crustal velocity discontinuities are significant indicators of the tectonic history of the lithosphere in a given region [*Chulick and Mooney*, 2002; *Gorman et al*., 2002; *Lekic et al*., 2011; *McGlannan and Gilbert*, 2016; *Parker et al*., 2013, 2015; *Rumpfhuber et al*., 2009; *Shen and Ritzwoller*, 2016; *Zheng et al*., 2015]. Figure 4a shows the depth of the Moho within the OIINK study area. Figure 4b shows the depth of the discontinuity in the broader CUS region. The reader can see the relationship of this surface to the full 3-D image volumes by viewing Movies S1 and S2. In general, the interpreted Moho surface is unusually deep (50 to 60+ km) in comparison to results of previous estimates (40 km to 45 km) derived from seismic reflection and refraction studies [*Catchings*, 1999; *Mooney et al*., 1983; *Okure and McBride*, 2006]. The results are similar, however, to the Moho depths of 45 to 55 km obtained by *McGlannan and Gilbert* [2016] using similar receiver function methods.

In the Ozark Dome region, the Moho surface is relatively shallow with a depth of around 45 km (Figures 4a and 4b), although this is significantly deeper than the average depth of about 36.1 ± 9 km for continental North America given by *Braile et al.* [1989]. The relatively shallower Moho in the Ozark region is a localized feature surrounded by a deeper Moho at its flanks (Figure 4b). In particular, the Sparta Shelf region east of the city of St. Louis, Missouri, has an extremely deep Moho with a depth of 57 to 62 km below sea level (Figures 4a and 4b). The transition from the Ozark Dome to the Sparta Shelf is defined by an abrupt boundary at the Moho interface located about 50 km to 70 km southwest of the SGFZ (Figure 4c), which lies roughly parallel to the Mississippi River. The deep Moho feature in the Sparta Shelf region terminates at the Sangamon Arch to the north and the Du Quoin Monocline to the east (Figures 4b and 4e). The Du Quoin Monocline defines the structural boundary between the Sparta Shelf and the Fairfield Basin. Beneath the Sparta Shelf region, there is a strong signal in the lower crust at a depth of about 30 km to 35 km (Figures 4e, 5b, and 5c). This signal extends about 70 km in the N-S direction (Figures 4e and 5c) and about 150 km in the NW-SE direction (Figure 5b), though it is not well imaged in the OIINK PWMIG result (Figure 4c). In addition, we notice a strong sub-Moho signal below the northwestern Illinois Basin to the north of the Sangamon Arch (Figures 4e, 4f, and 5c) and to the west of the La Salle Anticlinal Belt. This signal extends about 100 km to 120 km in a N-S direction and about 150 km to 200 km in an E-W direction (Figure 4b).

In the Rough Creek Graben area, the Moho depth is similar to that in the Ozark Dome region (Figure 4a). The Moho surface to the south of the Rough Creek Graben is also deeper than that within the graben (Figures 4b and 4g), although the surface is highly smoothed due to the large station spacing (about 70 km) in the CUS data set relative to the size of the Rough Creek Graben. The relatively shallow Moho in this region is confined within the rift zone with a relatively deeper Moho in areas flanking the rift proper (Figures 4b and 4g).

In summary, a relatively deep Moho dominates much of the Illinois Basin southeast of the Nd-line except for the Rough Creek Graben area (Figure 4b). The Moho reaches its maximum depth at the Sparta Shelf (Figures 4a and 4b). This region of deep Moho is bounded by the Pascola Arch to the southwest, the Grenville Front Tectonic Zone and the Appalachians to the southeast, the Kankakee Arch to the northeast, the Sangamon Arch and the La Salle Anticlinal Belt to the northwest, and the SGFZ to the west (Figure 4b). The Moho surface north of the Sangamon Arch is about the same depth as the Moho outside the Illinois Basin. Beneath the Ozark Dome away from its summit, the Moho interface is relatively flat in the SW-NE direction (Figure 4c), while dipping slightly to the W-NW ($<1.5°$) (Figure 5a), representing a thickened lower crust beneath the Nd-line.

3.2. Crustal Thickness

To analyze the dynamic processes associated with the variation of crustal thickness, it is helpful to isolate the crystalline crust from the overlying thick Phanerozoic sediments in the Illinois Basin. We derived the thickness

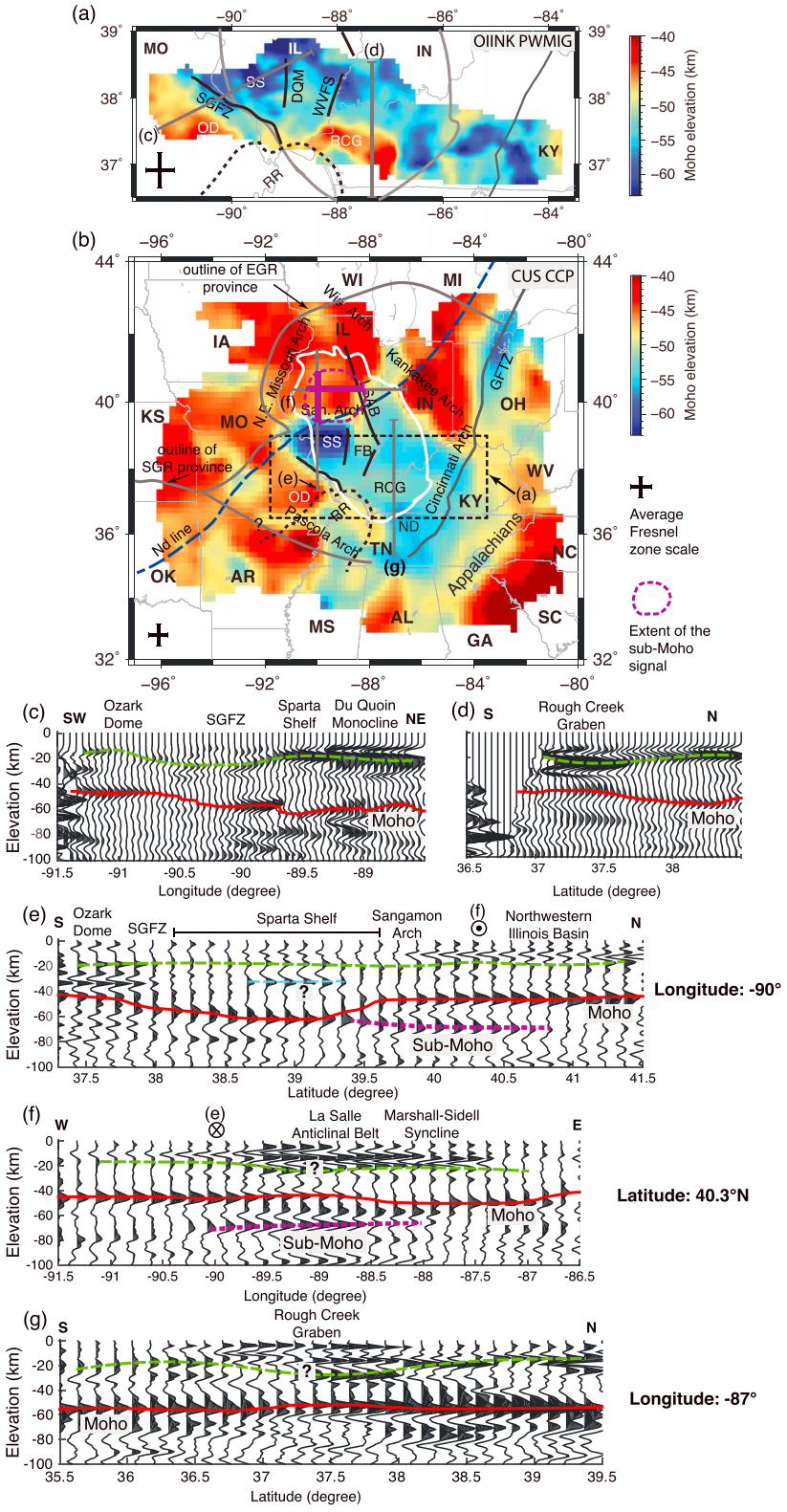

Figure 4. Moho depth maps from (a) OIINK PWMIG result and (b) CUS CCP stacking result. (c–g) Selected cross sections at locations shown in Figures 4a and 4b. The bin sizes for OIINK cross sections and for CUS cross sections are 5 km and 15 km, respectively. The red line in each cross section is the picked Moho surface. The green dashed lines are interpreted but not mapped crustal discontinuities. Structures shown are simplified from Figure 2. See Figure 2 for names (abbreviations) and locations of other major structures.

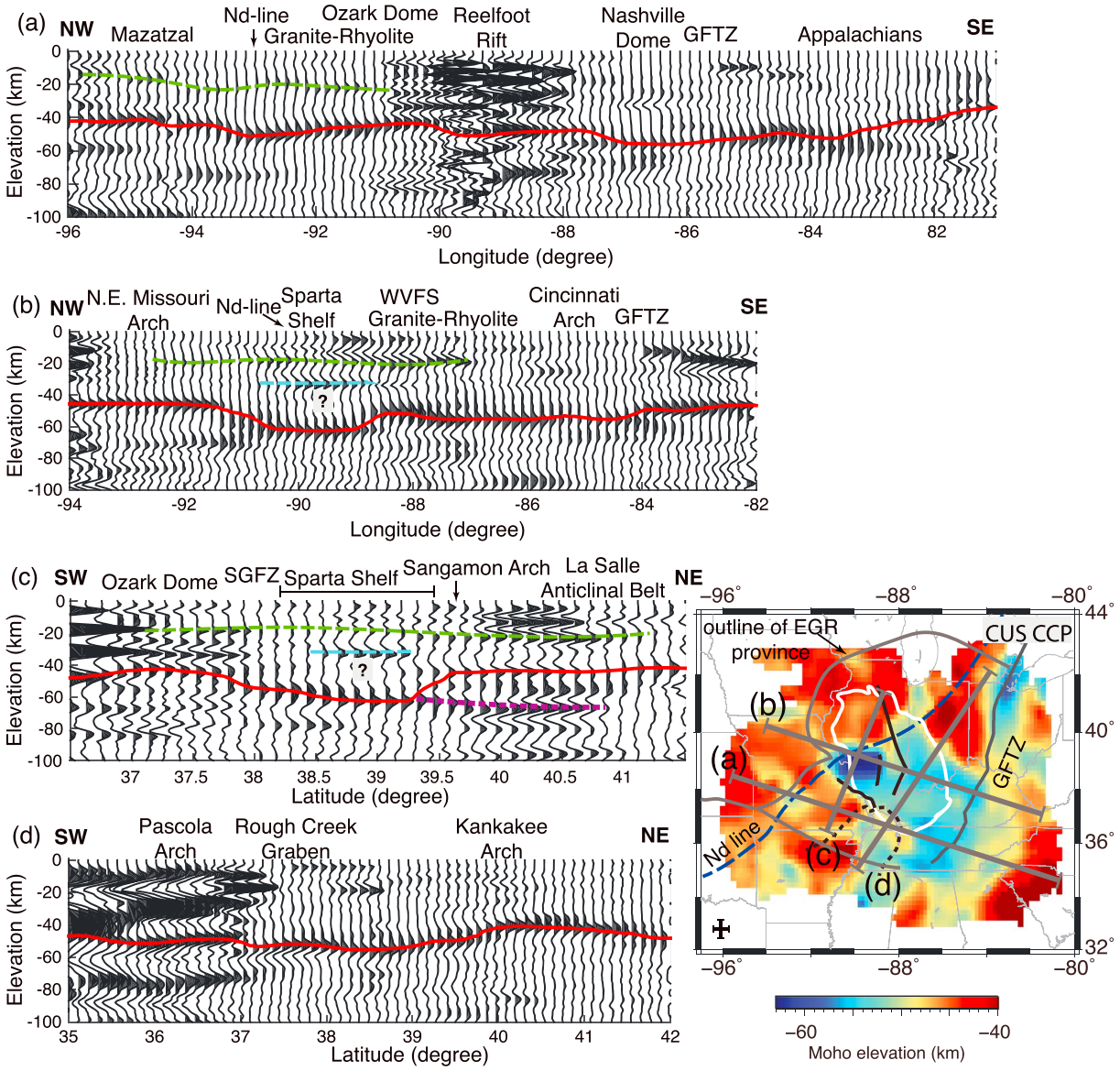

Figure 5. Selected regional cross sections of the CUS CCP stacking result. See the inset map for profile locations (see Figure 4b for names of major structures). (a, b, and d) There is a 2.5 times vertical exaggeration for cross sections. (c) The vertical exaggeration is 1.5 times.

of the crystalline crust in the OIINK and the CUS study areas (Figure 6) by subtracting the thickness of the Phanerozoic sediments, defined by depth of the Great Unconformity (see Figure 2), from the Moho depths (Figures 4a and 4b). For the rest of this paper we refer to "crustal thickness" as the thickness of crystalline crust defined by the isopach maps in Figure 6, distinguished from the Moho depths shown in Figures 4a and 4b.

The crustal thickness in the central Ozark Dome area is slightly less than that on its flanks (Figure 6), though comparable with the regional thickness (~40 km to 45 km) outside the Illinois Basin. From the Ozark Dome to the Sparta Shelf, the crust thickens drastically across the SGFZ, which is approximately parallel to the large gradient in crustal thickness. The Sparta Shelf region, with extremely deep Moho (57–62 km), is also characterized by localized thick crust (Figure 6). From the Sparta Shelf to the Fairfield Basin, variation of the crustal thickness follows the same pattern as that of the Moho elevation (Figures 4a and 4b).

The crustal thickness in the Rough Creek Graben region is about 35 km to 38 km. Compared to the surrounding areas, this thinner crust is confined within the rift zone and is bounded by the major faults in

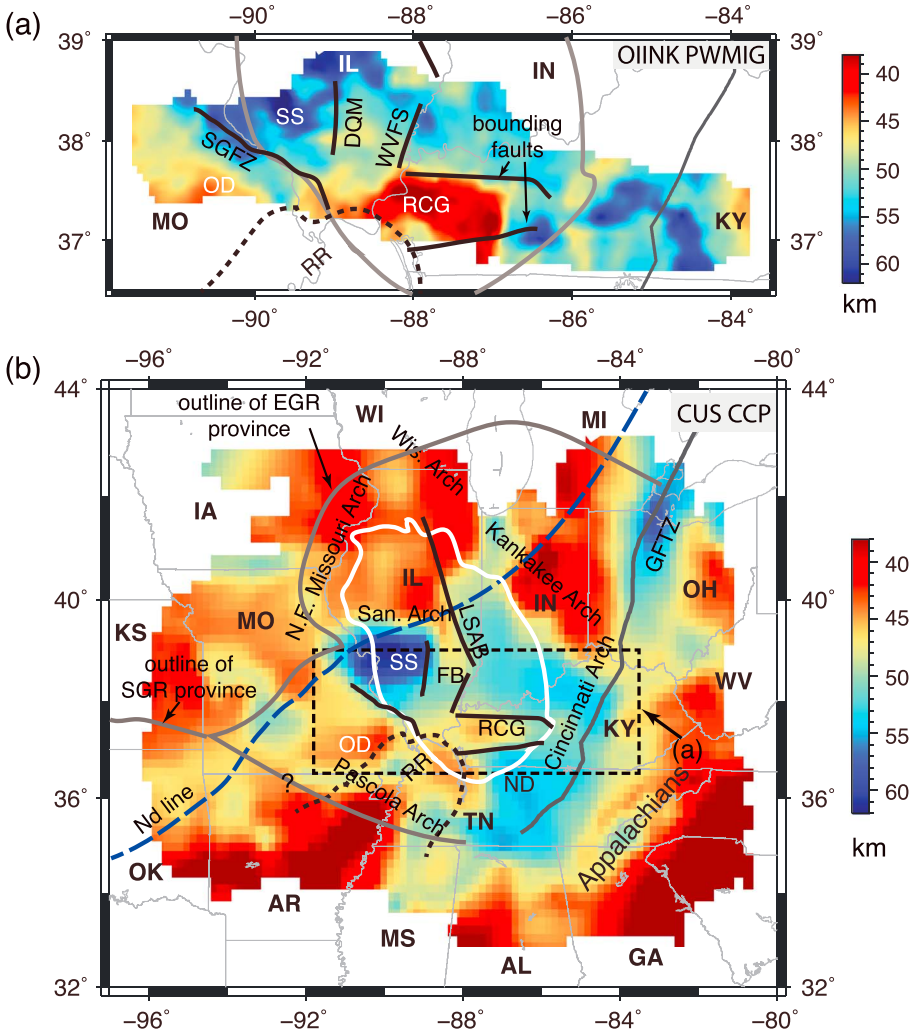

Figure 6. Derived isopachs of the crystalline crust (a) from the OIINK PWMIG Moho map and (b) the CUS CCP stacking Moho map. See Figures 2 and 4 for names and abbreviations of major structures.

its northern and southern flanks (Figure 6a). The result from CUS CCP stacking shows the same pattern with dramatically thinner crystalline crust within the rift zone and thicker crust flanking it (Figure 6b), highlighting the crustal thinning beneath the rifting structure compared to the Moho depth map (Figure 4b). The crustal structure beneath the Rough Creek Graben is similar to that beneath the La Salle Anticlinal Belt (Figures 4f and 4g).

Overall, the crystalline crust in the central and southeastern Illinois Basin is relatively thick in comparison to the surrounding regions, except for the regions around the Rough Creek Graben and west of the La Salle Anticlinal Belt, where we observe highly localized, relatively shallow Moho and thin crust. The crust is the thickest in the Sparta Shelf region, similar to the patterns observed in the Moho depth maps (Figure 4), bounded by three major cratonic structures: the Du Quoin Monocline to the east, the Sangamon Arch to the north, and the Ste. Genevieve Fault Zone to the southwest. Although the thick crust in the Sparta Shelf region appears to extend further southwest parallel to the surface trace of the Ste. Genevieve Fault Zone, the scale of this extension is comparable to the width of the Fresnel zone (Figure S3), and thus cannot be distinguished from a crustal thickness gradient coincident with the SGFZ.

3.3. Scattering Amplitudes

Scattering amplitudes are indicators of the velocity and/or density contrast across discontinuities. Values of the amplitudes of the receiver functions computed by the generalized iterative deconvolution [*Wang and*

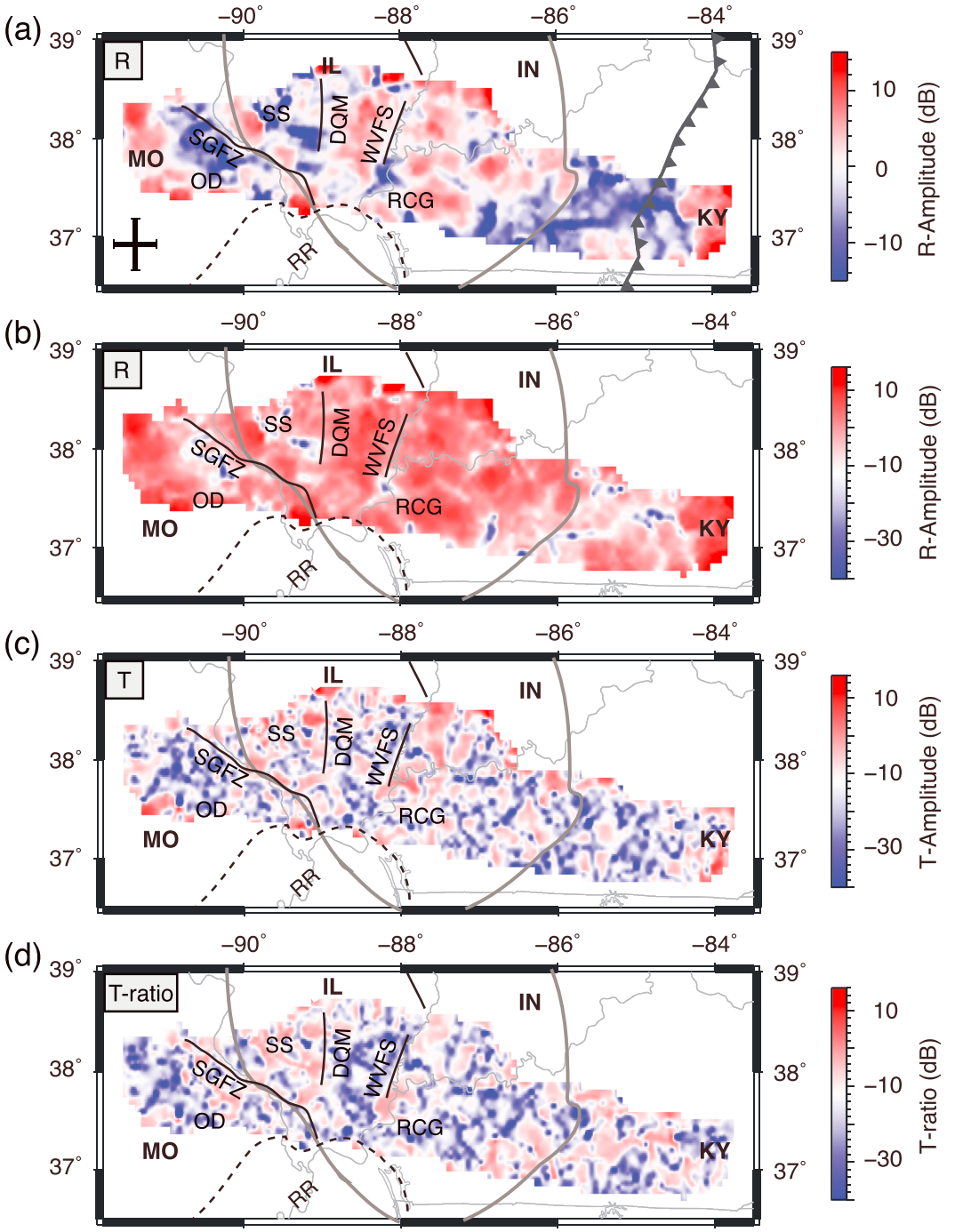

Figure 7. *P*-to-*S* conversion amplitudes at the Moho surface on (a and b) radial and (c) transverse components and the (d) *T*-ratio map from the OIINK PWMIG result. Figures 7a and 7b show the same information, but Figure 7a is scaled to maximize contrast while Figure 7b uses the same scale as Figure 7c to demonstrate variations in transverse amplitudes relative to radial. See Figures 2 and 4 for structure names and abbreviations.

Pavlis, 2016] are normalized amplitudes relative to the vertical component *P* wave. In this study, we use a power law gain function in depth with power of 1.4 to scale the scattering amplitudes (Text S3). In addition, we define *T*-ratio, or T_{ratio}, as the ratio of the amplitude of the total amplitude (Text S3).

The variation in *P*-to-*S* conversion amplitudes along a discontinuity reflects the variation of changes in wave speeds and density across the boundary. Figure 7 illustrates the *P*-to-*S* conversion amplitudes along the

picked Moho surface from the image volume of OIINK PWMIG. Considering the relatively poor amplitude recovery using CUS data, as we show in the next section, and for brevity, the CUS CCP stacking amplitudes are shown in Figure S5. The amplitude range of radial components is roughly −15 dB to +15 dB for both results.

The steeply dipping Moho transition zone between the Ozark Dome and the Sparta Shelf has relatively low radial amplitudes (Figures 7a and 7b). Simulation results (Texts S4 and S5) suggest that where steep velocity discontinuity surfaces are present amplitudes are commonly underestimated. This problem is more prevalent with CCP stacking compared to PWMIG [*Pavlis and Wang*, 2015]. Amplitudes of the transverse components (Figure 7c) are generally much lower and show stronger spatial variations than those of the radial components. The T_{ratio} map shows high anomalies along zones with steeply dipping Moho surface (Figure 7d). Dipping velocity interfaces produce azimuth-dependent amplitudes for seismic phases [*Schulte-Pelkum and Mahan*, 2014]. This results in relatively lower amplitudes along the direction closer to the strike of the dipping interface and is the likely reason for high T_{ratio} in these areas. Stacking-based seismic imaging methods provide average amplitudes for each image point which suppresses the azimuthal amplitude variation for each receiver. Therefore, the low radial amplitudes and increased transverse amplitudes are additional evidence that the steeply dipping Moho we infer in this area is real.

In the Sparta Shelf region, the amplitudes are relatively low compared to the surrounding regions such as the Fairfield Basin between the Du Quoin Monocline and the Wabash Valley Fault System (Figures 7 and S5). Although the amplitudes of transverse components are slightly higher in the Sparta Shelf region than the adjacent regions, the total scattered energy in this region is still lower than in surrounding regions (the map is not shown for brevity).

The overall amplitudes within the Rough Creek Graben are high and are similar to those in the Fairfield Basin area. We observe generally high conversion amplitudes in the region to the east of the Rough Creek Graben (Figure 7). This is not imaged very well in the CUS result (Figure S5) mainly due to the lower amplitude resolution in that result, as we demonstrate in the next section. As with the transitional zone between the Ozark Dome and the Sparta Shelf, the dramatic drop in the Moho elevation along the eastern edge of the Rough Creek Graben correlates with a region of relatively high *T*-ratios (Figure 7d).

4. Resolution Analyses

The imaging method we are using is a form of migration inversion [*Pavlis*, 2011b]. As with any inversion procedure, a critical component of the validation process is error appraisal. We applied the general method for appraising errors introduced by *Liu and Pavlis* [2013] to assess the resolving power of the results discussed above. The key concept is to produce a synthetic data set with the same recording geometry as the original data but computed from a known model. These synthetics are processed with exactly the same processing flow as the data. We generate synthetics from irregular surfaces by using a summation of point sources [*Liu and Pavlis*, 2013].

Checkerboard tests are a common tool used to appraise resolution in seismic tomography. In Text S4, we show the result of a similar concept, but with the checkerboard defined by a sinusoidal oscillation/surface around a constant depth Moho. The surface is approximated by point-source scatters on a regular grid [*Liu and Pavlis*, 2013]. We argue that the test results shown in Figures S6–S11 demonstrate the following key points: (1) OIINK imaging can accurately recover topography with dips up to around 20° and with horizontal scales larger than about 60 km (Figure S7). (2) The CUS data can resolve features on the order of 200 km and larger, but offsets in the Moho, like those parallel to the Mississippi River and on the edge of the Rough Creek Graben, are not resolvable with the CUS data alone (Figure S8). (3) The OIINK imaging can recover amplitudes with a range of about 12 dB (a factor of 4) (Figures S9–S11). (4) The CUS CCP stacking solution has an amplitude range of around 24 dB (a factor of 16). Amplitude variations in the OIINK image larger than around 10 dB are likely real. Amplitudes in the CUS image are subject to large errors where the Moho is dipping more than a few degrees across distance scales comparable to the TA station spacing of 70 km. When the Moho is flat the amplitudes are well recovered, though smoothed. As a result, we only show the amplitude results for the OIINK PWMIG solution, whereas simulations indicate that the CUS CCP amplitudes are unreliable.

In Text S5, starting with a representation of the estimated Moho topography, we verify how well we can recover that model in both topography and amplitude variations (Figures S12–S14). In addition, we have conducted detailed analyses of the impacts of sediments on our imaging results (Appendix A1) and the reliability of our Moho model (Appendix A2). These tests show that we can recover all of the major Moho variations with a depth uncertainty of about 2–3 km.

5. Discussion

5.1. Crustal Geometry of the Illinois Basin

Among the most unexpected observations is the thickness of the crust, which averages ~50 km, ranging from just over 40 km near the basin margins to as much as 62 km beneath the Sparta Shelf region. A thickness of 30–35 km is commonly presented as an average for continental crust globally. However, *Hacker et al.* [2015] have shown the global average for cratons to be ~40 km. The very thick crust we observe under the Illinois Basin is surprising, but not unprecedented. A 50 to 61 km thick crust was observed in the Proterozoic shield of central Australia by *Clitheroe et al.* [2000] and was attributed to underplating beneath it. *Wright et al.* [2004] estimated Moho depths of up to about 44 km to 51 km beneath the Kaapvaal craton in southern Africa that they also attributed to underplating. *Yu et al.* [2012] imaged the Moho at depths up to 60 km beneath the eastern Ordos Plateau in the north China craton and proposed that thick mafic lower crust helps maintain crustal isostasy. In the North American continent, *Gorman et al.* [2002] and *Rumpfhuber et al.* [2009] observed up to 55 km to 60 km thick crust, which they interpreted to have resulted from the addition of thick mafic lower crust, beneath the Wyoming craton, which terminates north of the Cheyenne Belt at latitude 42°N near the Rocky Mountain Front.

The large variations in crustal thickness are a particularly notable feature of our study area, given that this variation exists under an area with relatively little topographic relief. Specifically, there is only ~300 m of elevation difference between the highest point of the Ozark Dome in Missouri and the land surface over most of the Illinois Basin in Illinois. Comparison of the Moho depth map (Figures 4a and 4b) to topography of the Great Unconformity (the Precambrian/Paleozoic contact) [*Marshak et al.*, 2017] throughout the study area (Figure 2 and Movies S1 and S2) emphasizes that the depth variation in the Moho greatly exceeds that of the Great Unconformity. Thus, variation in Moho depth cannot simply be a consequence of downwarping of the crust during subsidence of the Illinois Basin. On the other hand, it is clear that the limits of the region of thicker crust partially coincide with the boundaries of the Illinois Basin (Figure 4b). Specifically, the southwest boundary lies along the NW trending boundary between the Ozark Dome and Illinois Basin, a feature that is delineated at the ground surface by the SGFZ [*DeLucia et al.*, 2016; *Yang et al.*, 2014]. The northeastern limit of thickened crust aligns with the southeastern edge of the Kankakee Arch, the northwestern limit coincides with the Nd-line defined by *Bickford et al.* [2015], and the southeastern edge parallels with the projected trace of the Grenville Front. These relationships imply that the presence of thicker crust may have influenced tectonic movements of the crust during episodes of cratonic basin subsidence and cratonic arch/dome uplift that took place during the Paleozoic.

5.2. Crustal Structure Associated With the Ste. Genevieve Fault Zone

The most profound crustal-scale structure inferred from this study is the dramatic offset of the Moho surface, up to 10 km, along the Missouri-Illinois border and the Mississippi River. This offset is spatially coincident with the SGFZ, suggesting that this fault zone is a surface manifestation of a profound crustal boundary connecting contrasting deep lithospheric structures on its two flanks. This offset of the Moho surface across the SGFZ occurs over a lateral distance of about 70–100 km (Figures 4a–4c). Resolution tests suggest that this offset is indistinguishable from a pure step. While the offset is also coincident with the steepest gradient in sediment thickness in the Illinois Basin, the Phanerozoic sediment thickness only increases by approximately 3 km eastward across this boundary (Figure S1b). There are two ways to explain the mismatch between the offset of the Moho surface and the thickness of the Phanerozoic sediments: (1) the Moho offset predates the subsidence of the Illinois Basin, which was focused along an existing zone of weakness, or (2) some process during the Late Precambrian to Early Cambrian rifting event, which produced the Reelfoot Rift and Rough Creek Graben, may have thickened the crust during rifting. In the next section, we argue that the latter is unlikely.

5.3. Rough Creek Graben-Reelfoot Rift Structure and Timing

The basement structure map in Figure 2, derived from the synthesis of decades of data collected by U.S. Geological Survey, state geologic surveys, and others, affirms the physical connection between the Rough Creek Graben and the Reelfoot Rift [e.g., *Braile et al*., 1982a, 1986, 1982b; *Hickman*, 2011; *Hildenbrand and Hendricks*, 1995; *Liang and Langston*, 2009]. The Reelfoot Rift is firmly established as a product of the latest Precambrian rifting event associated with the breakup of the supercontinent Rodinia [*Whitmeyer and Karlstrom*, 2007]. In the region of the Reelfoot Rift, *Mooney et al.* [1983] and *Nelson and Zhang* [1991] observed high-velocity lower crust in seismic refraction profiles that they interpreted as a "rift pillow" created by magmatic differentiation during the rifting event. *Liang and Langston* [2009] and *Chen et al.* [2016] confirmed the presence of high-velocity lower crust using tomographic techniques. The result from our study and some other recent studies [*McGlannan and Gilbert*, 2016; *Shen and Ritzwoller*, 2016] all show a relatively thin crust beneath the Reelfoot Rift and the Rough Creek Graben. The high-resolution result from the OIINK data (Figures 4a and 4c) shows this clearly when seen in the regional context of Figure 4b. The size of the Rough Creek Graben is comparable to the TA station spacing so our CUS results barely resolve this structure, while the higher-resolution OIINK data show a major offset in the Moho directly coincident with this structure. An important contribution of this study is to demonstrate a direct link between thinned crust under the Rough Creek Graben with a similar crustal thinning under the Reelfoot Rift.

Braile et al. [1982a, 1982b, 1986] introduced the concept of a three-arm rift structure linked to the Reelfoot Rift. Subsequent studies [*Catchings*, 1999; *Pratt et al*., 1989; *René and Stanonis*, 1995] have suggested that the shallow structural features associated with the St. Louis and Indiana Arms of the Reelfoot Rift complex are of much smaller scale than the well-documented rift structure associated with the Rough Creek Graben [*Kolata and Nelson*, 1997; *Nelson et al*., 1992; *Noger and Drahovzal*, 2005; *Wheeler*, 1997]. The St. Louis Arm, defined by *Braile et al.* [1982a, 1982b, 1986] as a rift extension following the strike of the Mississippi River between Missouri and Illinois, is coincident with the large Moho offset (5–10 km) discussed in section 5.2. Although similar velocity patterns are observed among these three arms in the lower crust and upper mantle [*Chen et al*., 2016; *Savage et al*., 2017], our results on the spatial distribution of crustal velocity discontinuities contradict the concept of the St. Louis and Indiana Arms. Specifically, both the localized, shallow Moho (Figure 4) and the confined, thin crystalline crust (Figure 6) suggest that rifting of the crust directly impacted only the areas of the Reelfoot Rift and Rough Creek Graben. The crust is significantly thinned under the Reelfoot Rift and Rough Creek Graben, but no such thinning is present along the areas hypothesized for the St. Louis or Indiana Arms. The low-velocity feature in the uppermost mantle coincident with both the New Madrid Seismic Zone and the Wabash Valley Seismic Zone inferred by *Savage et al.* [2017] may only indicate their similarity in seismogenic properties associated with the presence of low velocities. It is hard to conceive how the same process (i.e., rifting) operating in three areas would leave completely different Moho signatures with contrasting crustal thicknesses. Hence, we conclude that the hypothesis of a three-armed extension of the Reelfoot Rift is not supported by crustal thickness data. Our results provide direct evidence of only the eastern extension as the Rough Creek Graben. The localized rifting event under the Reelfoot-Rough Creek region modified only the crust and uppermost mantle in the vicinity of the rift, where the Illinois Basin sediments are the thickest.

5.4. Origin of the Midcontinent Cratonic Arches

The distribution and geometry of the cratonic arches in the region relative to the geometry of the Great Unconformity is shown in Figure 2 and Movies S1 and S2. The term Great Unconformity is used because of the extreme hiatus in geological record it represents for most of North America. In the region of Figure 2 that hiatus spans more than 600 Myr, from the end of the Grenville Orogeny to the Middle Cambrian. Thinning of the post-Ordovician sedimentary cover defines the arches themselves in comparison with adjacent basinal areas, indicating that the arches and basins were continuing to be positive features relative to deposition of Paleozoic sediments into the basin.

Our results show that the arches defining the outline of the Illinois Basin are coincident with areas of relatively normal-thickness continental crust, except for the Cincinnati Arch, which is residing within the deep Moho region (Figure 4). However, it is important to recognize that the scale of the offset along the Great Unconformity that defines the arches (1–2 km; Figure 2) is almost an order of magnitude smaller than the crustal thickness variations we infer here (5–10 km; Figure 6). This contrast in scales suggests strongly that

the arches were localized by preexisting geometry and are not the cause of crustal thickness variations themselves. Some other process must have created the variations in crustal thickness beneath these arches and the entire study area.

5.5. Precambrian History That Shaped the Illinois Basin

We infer that much of the anomalously thick crust we observe for the midcontinent is inherited from previous tectonic events. What process then could have created this unusual crustal geometry? To address that question, we first review some critical points about current understanding of the nature of continental crust.

Concepts of gross structure of the crust have been strongly shaped by seismic refraction measurements that lump the crust into a near-surface sedimentary layer, an upper, presumably felsic, crust, and a lower, presumably mafic, crust. The widely used global compilation of Crust2.0 [*Bassin et al*., 2000] implicitly forces this structure into their model. However, as noted by *Hacker et al.* [2015], this seismically distinct layering is not a universal feature of continental crust, and interpretation of such layers should be done with caution. Instead, they argue that the lower part of the continental crust, in particular, could be composed of very different lithologies in different areas and could have formed due to a range of processes. In cratons, the lower crust could have small density contrasts with the underlying mantle or even be gravitationally unstable and remain in place because of the thick lithosphere of the craton [*Hacker et al*., 2015]. This could explain why the observed gravity in the region (Figure S1a) has little correlation with our Moho structure map (Figure 4). *Yang* [2016] used simple 2-D modeling to show that realistic lateral density variations for the lower crust and upper mantle could be used to match gravity profiles perpendicular to Missouri-Illinois border. Future work is needed to constrain density variations within the crust that can simultaneously explain the detailed characteristics of the measured gravity field. Nonetheless, our current understanding of the nature of the lower crust [*Hacker et al*., 2015] suggests that a reasonable distribution of known rock assemblages is feasible to reconcile both observations.

We argue that the general Moho geometry seen in Figure 4 must have been created in the Precambrian prior to the formation of the Illinois Basin. To articulate how our results could be related to the earlier geologic history, we jump backward to the time of formation of the crust in this region and then work our way forward to appraise what events may have created the observed crustal geometry.

Our study area spans two terranes of Precambrian crust underlying the area (Figure 1), commonly called the Mazatzal Province and the EGRP. *Whitmeyer and Karlstrom* [2007] link the Mazatzal to a terrain accretion, the Mazatzal Orogeny, which occurred between 1.65 and 1.6 Ga (Table 1). The EGRP rocks overlie the Mazatzal in the study area in a manner that is not well constrained because the only exposure of EGRP rocks is in the Ozarks and in sparsely distributed boreholes elsewhere in the region. *Bickford et al.* [2015] provide a recent review of what is known about the EGRP. The Nd-line across the EGRP (Figure 1) marks a boundary with Nd age greater than 1.55 Ga to the northwest and younger to the southeast [*Whitmeyer and Karlstrom*, 2007], suggesting two distinct episodes of formation. The entire midcontinent was tectonically active in the period from 1.65 to 1.35 Ga (Table 1). Hence, one hypothesis to explain the crustal structure we observe is that geologic processes in the period of 1.65 to 1.35 Ga created this crust and/or modified it into this geometry. For example, the metamorphic history of garnet samples collected within the Mazatzal terrane in the southwestern United States indicates the presence of thickened crust during the Mesoproterozoic [*Aronoff et al*., 2016]. Because the timing of metamorphism was outside of the period of other orogenic episodes [*Aronoff et al*., 2016], this metamorphism has been attributed to compression during the "Picuris Orogeny" around 1490 Ma–1450 Ma, named after the Picuris Mountains of northern New Mexico [*Daniel et al*., 2013]. The presence of thickened crust resulting from compressional tectonics may similarly explain the broad swath of thickened crust trending along the Mazatzal and the EGRP across the central and eastern United States [*Shen and Ritzwoller*, 2016].

This area was likely to have been affected by a series of later events from 1.3 to 0.9 Ga associated with the Grenville Orogeny, which culminated in the assembly of the supercontinent Rodinia [*Whitmeyer and Karlstrom*, 2007]. *Whitmeyer and Karlstrom* [2007] describe this period as a history of accretionary orogenesis along an east and southeast facing, predominantly convergent, margin. During this episode of extended compression, the midcontinent was also impacted by the contemporaneous rifting episode that produced the Midcontinent Rift [*Whitmeyer and Karlstrom*, 2007]. *Hauser* [1996] suggests that this rifting event was

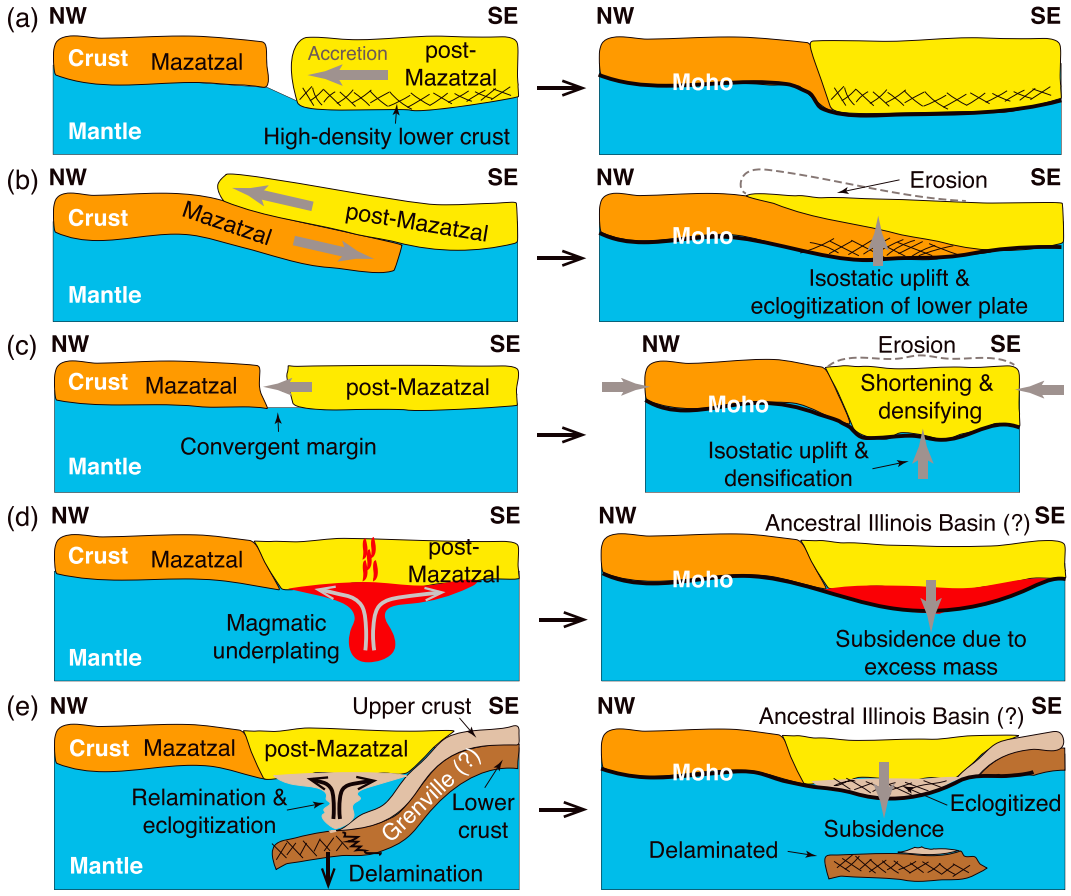

Figure 8. Cartoons illustrating the proposed hypotheses to explain the observed thick crust in central and southeastern Illinois Basin area: (a) inherited thick crust from terrane accretion (hypothesis 1), (b) thickening through underthrusting at convergent margins (hypothesis 2), (c) thickening through shortening of the overriding plate at convergent margins (hypothesis 2), (d) thickening due to magmatic underplating (hypothesis 3), and (e) thickening by relamination of the lighter upper crust of the downgoing plate (hypothesis 4). These cartoons are not to scale. For each hypothesis, the left plot shows the proposed process (scenario), while the right plot shows the resultant crustal structure as observed at present. For simplicity, crustal layering is not shown for the Mazatzal and Granite-Rhyolite terranes, except for the subducting crust in Figure 8e.

analogous to rifting seen today in the Middle East created by block rotation of the Arabian plate. Except for the Ozarks, the Precambrian rocks of this entire area are all in the subsurface and known only by limited borehole data and inferences from geophysical data [*Marshak et al.*, 2017]. Hence, the details of how Proterozoic orogenic events might have modified the crust is not well constrained. We can at best outline processes that may have contributed to the production of thickened cratonic crust in the Illinois Basin region.

5.6. Hypotheses to Explain Crustal Thickening in the Illinois Basin

We observe anomalously thick crust in most of the central and southeastern Illinois Basin area, with strong variations in thickness with respect to the broader North American Midcontinent. The region of anomalously thick crust is bounded by the SGFZ, the Ozark Dome, and the Pascola Arch to the southwest, the Sangamon Arch and the NE Missouri Arch to the northwest, the Kankakee Arch to the northeast, and the Appalachians to the southeast. We argue that formation of this thick crust predates and may have contributed to the formation and development of the present Illinois Basin. Although we are yet unable to determine a single, unique model from currently available data, we examine four hypotheses to explain the observed thick crust (Figure 8).

Hypothesis 1: the thick crust was an inherited feature of the crust when it accreted to North America (Figure 8a).

The boundary between the Mazatzal terrane and the younger terrane to the southeast (post-Mazatzal terrane) depicted by *Whitmeyer and Karlstrom* [2007] aligns approximately with the northwestern limit of

the thickened crust imaged here. One explanation of this coincidence is that the younger crust was already anomalously thick when it accreted to the Mazatzal during the period of 1.55–1.35 Ga. Furthermore, the lower crust of this accretionary terrane should have high-density materials to maintain gravitational equilibrium and to match the present pattern of gravity anomalies, as suggested by *Yang* [2016]. If this is true, the thick crust we observed in central and southeastern Illinois Basin area was inherited from the process that originally created the post-Mazatzal terrane. The Reelfoot Rift-Rough Creek Graben was formed subsequently by rifting and localized thinning of this thickened crust in Late Precambrian to Early Cambrian time, which may have triggered the formation of the neighboring Illinois Basin [*Kolata and Nelson*, 1997].

Hypothesis 2: the crust was thickened through processes of shallow underthrusting (Figure 8b) or shortening (Figure 8c) of the crust under convergent margin tectonics.

Two processes have been suggested for large-scale thickening of crust at convergent margins: (1) thickening resulting from an episode of shallow underthrusting (Figure 8b), as has been suggested for the Tibetan Plateau [e.g., *Zhao and Nelson*, 1993], or (2) shortening and thickening of the overriding plate during convergence (Figure 8c), as identified in the modern western margin of South America [e.g., *Ward et al*., 2013]. Surface erosion and isostatic uplift could be consequences of both of these two thickening processes (Figures 8b and 8c), which could have occurred either during Proterozoic terrane accretion (1.55–1.35 Ga) or during the subsequent Grenville Orogeny (1.3–1.09 Ga). Within the thickened crust, lower crustal materials would be subjected to high-pressure conditions during continental convergence, which in turn might cause them to be metamorphosed into eclogites (Figure 8b). The transformation to eclogite is known to be associated with an increase in density and seismic wave velocities [*Ringwood and Green*, 1966]. The increased densities of the eclogites in the lower crust could then cause subsidence of the surface and the formation of a basin on the top. However, the sluggish kinetics of the eclogite phase transition often delays the formation of eclogites, even while being subjected to *P-T* conditions within the eclogite stability field [*Hacker*, 1996]. Instead, the lower crustal material remains untransformed until the introduction of fluids or an increase in temperature at some later time catalyzes the transformation to eclogite [*Hacker*, 1996]. Eclogite has an impedance more similar to mantle than to crust, which would reduce the *P*-to-*S* conversion amplitudes. From our simulation tests, the CUS amplitudes from the real data are unreliable, prevents us from comparing the overall amplitudes associated with the thick crust region in central and southeastern Illinois Basin with other regions. Thus, we cannot preclude the possibility of eclogitization at the base of the crust.

Hypothesis 3: the crust was thickened by Late Precambrian magmatic underplating beneath the crust (Figure 8d).

Magmatic underplating is a process that has been suggested to explain thickening of continental crust during rifting events [e.g., *Thybo and Artemieva*, 2013]. This process adds excess mass to the crust, resulting in gravitational subsidence of the crust due to negative buoyancy (Figure 8d). The surface subsidence associated with this process could have created accommodation space for the Illinois Basin. The most likely rift event that could have thickened the crust in this manner is the Latest Precambrian rifting (around 550 Ma) that created the Reelfoot Rift-Rough Creek Graben structure. This rifting seems to have produced focused deformation that followed the maximum subsidence of the crust under the Reelfoot Rift and Rough Creek Graben. However, we know of no documented process that could simultaneously thin the crust under narrow tectonic zones and underplate the crust regionally by orders of magnitude larger volumes to produce the thickened crust. An alternative source for underplating, which we see as more viable, is the voluminous magmatism that produced the EGRP. Given the geographic scope and the range of tectonic models proposed for the EGRP [*Bickford et al*., 2015], an underplating model is certainly viable. An important inconsistency in such a model, however, is that the major crustal boundary along the Missouri-Illinois border we imaged here crosscuts the mapped extent of the EGRP.

Hypothesis 4: the thick crust was a result of crustal "relamination" under convergent conditions, possibly associated with Proterozoic flat-slab subduction beneath the Illinois Basin (Figure 8e).

Another mechanism to thicken the crust is a set of convergent boundary processes illustrated in *Hacker et al.* [2015] that they refer to as "relamination," a corollary to the process of delamination. In this hypothesis, the more buoyant, felsic crustal material is separated from a downgoing plate after subduction and becomes amalgamated with the upper plate above it [*Hacker et al*., 2015]. This convergent process might be related

to a Proterozoic flat-slab subduction zone, possibly associated with the Grenville Orogeny, beneath the Illinois Basin region, as proposed by *Bedle and van der Lee* [2006]. The relaminated crust of the downgoing plate, after accreting to the upper plate, would be hypothesized to then undergo eclogization and produce subsidence due to the resulting increase in density, similar to *hypothesis* 3. This process may have formed an ancestral Illinois Basin (Figure 8e). Even though our data cannot provide timing information of this relamination process, we suggest that the most likely time period of this process was during the Grenville Orogeny. Given that the long axis of the thickened crust area we infer here (Figure 6) is approximately perpendicular to the Grenville Front (roughly NW-SE), the Grenville Orogeny appears to be a likely candidate.

Any model for crustal evolution of the North American craton must address the unambiguous evidence for thickened and highly variable crust in the U.S. midcontinent. We believe the four hypotheses discussed above all offer feasible mechanisms to explain the observed thickening of the crust under the Illinois Basin. Each hypothesis carries strengths and limitations; ultimately, resolution of these competing models will rely on additional constraints on crustal architecture beneath the craton. *Hypothesis* 1 attributes the thick crust to be an inherited feature of the accreted post-Mazatzal crust. Further investigations on detailed geometry and evolution of this thick crust prior to its accretion to the Mazatzal terrane are needed to test its feasibility. Underthrusting of the Mazatzal terrane beneath the post-Mazatzal terrane during continental collisions (*hypothesis* 2; Figure 8b) could explain the observed deep Moho and thick crust but lacks any observation of an eastward dipping underthrust Mazatzal crust. Alternatively, such a suture may have been modified during subsequent evolution of the crust and is thus not observable in receiver function images. Future kinematic studies would be helpful in validating this process. Shortening and thickening during convergent margin tectonics of *hypothesis* 2 (Figure 8c) could explain the slightly deformed crustal discontinuities, though it is not clear how this process would have been localized in the central and southeastern Illinois Basin instead of widely spread parallel to the compressional front. *Hypothesis* 3 supports the observations in Moho geometry, crustal thickness variation, and crustal velocity structure. However, more robust gravity modeling would be helpful to examine the feasibility of this hypothesis in matching the Bouguer gravity to seismic structure in this area (Figure S1a). The crustal relamination process of *hypothesis* 4 explains the current observations on Moho geometry, crustal thickness, and crustal velocity structure. However, we need more evidence to test the existence of a flat-slab subduction beneath this area as well as its timing relationship with the crustal thickening due to relamination in this region.

6. Conclusion

In this study, we present new results from a regional study of the lithospheric structure along a swath from Missouri to central Kentucky crossing the Illinois Basin. We imaged the crust-mantle boundary (Moho surface) across the southern Illinois Basin using both common conversion point stacking and plane wave migration methods. We evaluated the imaging results through extensive simulation tests.

Our imaging results reveal surprisingly large variations in crustal thickness within this part of the Central U.S in comparison to topographic relief of the region. The imaging also showed coincidence of features in the crust and uppermost mantle with major structures in the study area, including the Ozark Dome, the Sparta Shelf, the SGFZ, the Reelfoot Rift, and the Rough Creek Graben. We find an exceptionally deep Moho (~50–62 km) throughout the center of the study area roughly centering on the southern Illinois Basin. The region of thickened crust is bounded by the SGFZ, the Ozark Dome, and the Pascola Arch to the southwest, the Sangamon Arch and the NE Missouri Arch to the northwest, the Kankakee Arch to the northeast, and the Appalachians to the southeast. The crust is thickest in this area at the Sparta Shelf region, with a Moho depth of about 55–62 km.

Our results show a profound crustal-scale boundary parallel to the Ste. Genevieve Fault Zone near the Illinois-Missouri border, where the depth to Moho increases from around 45 km under the Ozarks to over 60 km beneath the Sparta Shelf region. This offset is sharp and indistinguishable from a step within the resolution of our imaging. This boundary is spatially coincident with the steepest gradient in sediment thickness in the Illinois Basin, exceeding the offset in the Precambrian-Cambrian boundary by a factor of about 3.

We image another dramatic offset in crustal thickness that corresponds with bounding faults of the Rough Creek Graben, which is the eastern extension of the Reelfoot Rift. We argue that the structural relation of these two major offsets leads to two conclusions about the geologic history of this rift structure: (1) the

Rough Creek Graben is a structural extension of the Reelfoot Rift and (2) the rifting event that produced the Reelfoot Rift-Rough Creek Graben and subsequent subsidence that formed the Illinois Basin may have overprinted crust that was already anomalously thick. The crustal structure from this study indicates that the SGFZ and the Reelfoot Rift-Rough Creek Graben structure are the surface manifestations of profound crustal-scale structural boundaries across which the crustal thickness changes dramatically.

We examine four hypotheses to explain the existence of thick crust in the Illinois Basin area: (1) an inherited feature of the crust when it accreted to North America; (2) thickening through shallow underthrusting or shortening of the crust under convergent margin tectonics; (3) thickening due to Late Precambrian magmatic underplating beneath the crust; and (4) a result of crustal relamination under convergent environment, possibly associated with Proterozoic flat-slab subduction beneath the Illinois Basin.

7. Data and Resources

The USArray arrival time data set was downloaded from the EarthScope Array Network Facility (http://anf.ucsd.edu, last accessed February 2017). Waveforms linked to these arrivals were assembled from the Incorporated Research Institutions for Seismology Data Management Center. The OIINK data set is archived under the network code XO_2011: http://www.fdsn.org/networks/detail/XO_2011/. Information about other networks involved in this study can be found from the following resources: Cooperative New Madrid Seismic Network (http://www.eas.slu.edu/eqc/eqcnetinfo.html, last accessed February 2017) and Global Seismographic Network (GSN) (http://earthquake.usgs.gov/monitoring/gsn, last accessed February 2017).

We used the Generic Mapping Tools (http://gmt.soest.hawaii.edu/, version 4.5.7, last accessed February 2017) to produce all of the maps (except for cross sections) in this study. We used the *ParaView* software package [*Ayachit*, 2015] in making the Movies S1 and S2. The source code of the computer program, *RFeditor*, used in receiver function quality control is available from https://github.com/xtyangpsp/RFeditor (last updated February 2017). The Bouguer gravity anomaly data for the CUS region were downloaded from http://topex.ucsd.edu/cgi-bin/get_data.cgi (last accessed on February 2017).

Appendix A

A1. Impacts of Sediments

As is typical of most basins, the sediments of the Illinois Basin have complexity at all scales, but have a fundamental layering that is well captured in the basin model we used for computing statics. A more difficult problem to handle is that of sediment reverberations, as analyzed in previous studies [e.g., *Langston*, 2011; *Tao et al.*, 2014; *Yu et al.*, 2015]. Sediment reverberations might be expected to contaminate all of these data to some degree.

Figures S5a and S5d show that within the northern Mississippi Embayment area, where we have relatively low data coverage (Figure S4b), the *P*-to-*S* conversions from the Moho surface are strongly contaminated by reverberations from shallow sediments. Thus, the image we constructed in the Mississippi Embayment area is unreliable.

In contrast, the Phanerozoic carbonate sediments that fill much of the Illinois Basin have relatively high velocities (Table S3). This property ensures that the sedimentary reverberations in this area are minimal and impact only the uppermost part of the image. *Yang* [2016] demonstrated this by running simulations of the basin model that included all reverberations and processing the results as in the checkerboard tests. He found that sediment reverberations associated with the Illinois Basin area do not have pronounced impact on the Moho signal. This implies that the Moho surfaces from the real data (Figure 4) in our study are not as sensitive to seismic reverberations associated with the sedimentary layers of the Illinois Basin as they are in the Reelfoot Rift area.

A2. Reliability of Moho Depth Estimates

The $>$50 km deep Moho we estimate for the Sparta Shelf region and other regions in the south-central Illinois Basin area is much deeper than some previous estimates. *Catchings* [1999] revealed a northward thickening middle crust north of the SGFZ, a nearly flat Moho at the depth of 42–43 km, and an upper mantle discontinuity at the depth of 60 km along a seismic profile from Memphis, Tennessee to St. Louis, Missouri. Geometry of the Moho surface from our study has a similar, though much deeper, pattern with that of the base of the

middle crustal layer along the S-N profile by *Catchings* [1999]. The lower crust above the nearly flat Moho thins dramatically north of the SGFZ [*Catchings*, 1999]. It is not clear, however, why such strongly deformed crustal structures are underlain by flat uppermost mantle layers. *Okure and McBride* [2006] interpreted a 38 km deep Moho and sub-Moho reflectors in the uppermost mantle between depths of 40–60 km in southern Illinois Basin based on seismic reflection profiles, though the Moho signals are highly occasional. We argue that the Moho signals interpreted by *Okure and McBride* [2006] might be from isolated crustal scatters, while the upper mantle reflectors they observe might be more related to the Moho signals we interpreted from the images in this study. We argue that the interpretation of a flat Moho may oversimplify the Moho geometry in the Illinois Basin area. In addition, our results indicate significant topography on the Moho surface, which cannot be explained if the Moho were interpreted to be flat. *McGlannan and Gilbert* [2016] provide a Moho depth map in the similar area around the Illinois Basin using CCP stacking of teleseismic *P* wave receiver functions. While sharing some major features with our Moho map, our use of more detailed velocity structure during the time-to-depth migration and the accounting for the effects of shallow sediments help produce a higher-resolution map of Moho depths, especially in the OIINK study area. We evaluated the reliability of our Moho surface through intensive resolution tests. A similar Moho geometry revealed by *S* wave receiver functions [*Chen et al*., 2017] argues that neither observation can be simply attributed to a processing artifact. A more extensive comparison of the *P*-to-*S* receiver function and *S*-to-*P* receiver function results is beyond the scope of our paper, but merits further examination.

The Moho depth map of our study area in the Central United States given by *Shen and Ritzwoller* [2016] has patterns similar with our results, though their Moho estimates are generally shallower. For instance, in the Sparta Shelf region, they estimate that the Moho is about 46 km to 48 km deep. However, the standard deviations of the Moho depth in this area from their study are estimated to be in the range of about 5 km to 6 km. Moreover, the lateral resolution of their Moho depth result is much lower than ours, suggesting that their result could overlook a feature of this size due to smoothing. Uncertainties of the Moho surface mainly come from sources including (1) irregular data coverage, (2) errors in the migration velocity model, and (3) errors in picking the surface. Although there is no quantitative uncertainty analysis in our study, the Moho recovery test results (Text S5 and Figure S12) suggest depth recovery errors of no more than ±2 km around the Moho surface. For the OIINK results (Figures S12c and S12f), most of the depth recovery errors are within ±1 km. We conclude that the data coverage is sufficient in our study area to conclude that all but the shortest-wavelength features are real. From our complete suite of tests (Figure S15), there is a 2 km to 3 km depth variation using the various velocity models available for the southern Illinois Basin area [*Kennett and Engdahl*, 1991; *Kennett et al*., 1995; *Langston*, 1994]. We utilized the latest velocity model available for the Central U.S. by *Chen et al.* [2016] and incorporated the high-resolution basin model from *Ellett and Naylor* [2016] through static corrections, minimizing the uncertainties caused by migration velocities.

Acknowledgments

The data used in this study are listed in the supporting information and the website links described in detail in section 17. Instrumentation for the OIINK experiment was provided by the PASSCAL Instrument Center of the IRIS Consortium. The OIINK experiment was supported by the National Science Foundation (NSF) grants EAR-1053354 to Indiana University, EAR-1053248 to Purdue University, and EAR-1053551 to the University of Illinois under the EarthScope program. Data used in this project were accessed from the Incorporated Research Institutions for Seismology (IRIS) Data Management Center. Data from the TA network were made freely available as part of the EarthScope USArray facility, operated by IRIS and supported by the National Science Foundation, under cooperative agreement EAR-1261681. IRIS Data Services are funded through the Seismological Facilities for the Advancement of Geoscience and EarthScope (SAGE) Proposal of the National Science Foundation under cooperative agreement EAR-1261681. We thank Schlumberger Corporation for a software grant to allow use of the Petrel interpretation software. Special thanks to all the OIINK team members, especially to our supertechnician Terry Stigall and the dozens of student participants from three institutions, for their contributions to the deployment and operation of OIINK stations. We thank Southern Illinois University and the Kentucky Geological Survey for the logistical and facilities support during our field deployments. We are especially grateful to all the landowners for allowing us to install and operate stations on their properties. Computing resources for this project were partly supported by the Lilly Endowment, through its support for the Indiana University Pervasive Technology Institute, and in part by the Indiana METACyt Initiative. Thanks to Kevin Ellett for providing the 3-D structure model for the Illinois Basin. We appreciate the constructive comments and reviews from Seth Stein and another anonymous reviewer that have greatly improved the manuscript.

References

Aronoff, R. F., C. L. Andronicos, J. D. Vervoort, and R. A. Hunter (2016), Redefining the metamorphic history of the oldest rocks in the southern Rocky Mountains, *Geol. Soc. Am. Bull.*, *128*(7-8), 1207–1227, doi:10.1130/B31455.1.

Ayachit, U. (2015), The ParaView guide: A parallel visualization application, edited, Kitware.

Baranoski, M. T., S. L. Dean, J. L. Wicks, and V. M. Brown (2009), Unconformity-bounded seismic reflection sequences define Grenville-age rift system and foreland basins beneath the Phanerozoic in Ohio, *Geosphere*, *5*(2), 140–151, doi:10.1130/Ges00202.1.

Bassin, C., G. Laske, and G. Masters (2000), The current limits of resolution for surface wave tomography in North America, *Eos Trans. AGU*, *81*, F897.

Bayley, R. W., W. R. Muehlberger, and Geological Survey (U.S.) (1968), Basement rock map of the United States, exclusive of Alaska and Hawaii, Geological Survey, Washington, D. C.

Bedle, H., and S. van der Lee (2006), Fossil flat-slab subduction beneath the Illinois Basin, USA, *Tectonophysics*, *424*(1-2), 53–68, doi:10.1016/j.tecto.2006.06.003.

Bickford, M. E., W. R. Van Schmus, and I. Zietz (1986), Proterozoic history of the midcontinent region of North America, *Geology*, *14*(6), 492–496, doi:10.1130/0091-7613(1986)14<492:Photmr>2.0.Co;2.

Bickford, M. E., W. R. Van Schmus, K. E. Karlstrom, P. A. Mueller, and G. D. Kamenov (2015), Mesoproterozoic-trans-Laurentian magmatism: A synthesis of continent-wide age distributions, new SIMS U-Pb ages, zircon saturation temperatures, and Hf and Nd isotopic compositions, *Precambrian Res.*, *265*, 286–312, doi:10.1016/j.precamres.2014.11.024.

Braile, L. W., W. J. Hinze, G. R. Keller, and E. G. Lidiak (1982a), The northeastern extension of the New Madrid seismic zone, in Investigations of the New Madrid, Missouri, earthquake region, edited by F. A. McKeown and L. C. Pakiser, *U.S. Geol. Surv. Prof. Pap.*, *1236*, 175–184.

Braile, L. W., G. R. Keller, W. J. Hinze, and E. G. Lidiak (1982b), An ancient rift complex and its relation to contemporary seismicity in the New Madrid seismic zone, *Tectonics*, *1*, 225–237.

Braile, L. W., W. J. Hinze, G. R. Keller, E. G. Lidiak, and J. L. Sexton (1986), Tectonic development of the New Madrid Rift Complex, Mississippi Embayment, North America, *Tectonophysics*, *131*, 1–21.

Braile, L. W., W. Hinze, R. R. B. von Frese, and G. R. Keller (1989), Seismic properties of the crust and uppermost mantle of the conterminous United States and adjacent Canada, *Geol. Soc. Am. Mem.*, *172*, 655–681.

Buschbach, T. C., and D. R. Kolata (1991), Regional setting of Illinois Basin, in *Interior Cratonic Basins*, edited by M. W. Leighton et al., *AAPG Mem.*, *51*, 29–55.

Catchings, R. D. (1999), Regional V_p, V_s, V_p/V_s, and Poisson's ratios across earthquake source zones from Memphis, Tennessee, to St. Louis, Missouri, *Bull. Seismol. Soc. Am.*, *89*(6), 1591–1605.

Chen, C., H. Gilbert, C. Andronicos, M. W. Hamburger, T. Larson, S. Marshak, G. L. Pavlis, and X. T. Yang (2016), Shear velocity structure beneath the Central United States: Implications for the origin of the Illinois Basin and intraplate seismicity, *Geochem. Geophys. Geosyst.*, *17*, 1020–1041, doi:10.1002/2015GC006206.

Chen, C., H. Gilbert, K. M. Fischer, C. L. Andronicos, G. L. Pavlis, M. W. Hamburger, S. Marshak, T. Larson, and X. Yang (2017), Lithospheric discontinuities beneath the US Midcontinent—Signatures of Proterozoic terrane accretion and a failed rift, paper presented at EarthScope National Meeting, Anchorage, Alaska, 16-18 May.

Chu, R. S., and D. Helmberger (2014), Lithospheric waveguide beneath the Midwestern United States; massive low-velocity zone in the lower crust, *Geochem. Geophys. Geosyst.*, *15*, 1348–1362, doi:10.1002/2013GC004914.

Chulick, G. S., and W. D. Mooney (2002), Seismic structure of the crust and uppermost mantle of North America and adjacent oceanic basins: A synthesis, *Bull. Seismol. Soc. Am.*, *92*(6), 2478–2492, doi:10.1785/0120010188.

Clitheroe, G., O. Gudmundsson, and B. L. N. Kennett (2000), The crustal thickness of Australia, *J. Geophys. Res.*, *105*, 13,697–13,713, doi:10.1029/1999JB900317.

Daniel, C. G., L. S. Pfeifer, J. V. Jones, and C. M. McFarlane (2013), Detrital zircon evidence for non-Laurentian provenance, Mesoproterozoic (ca. 1490–1450 Ma) deposition and orogenesis in a reconstructed orogenic belt, northern New Mexico, USA: Defining the Picuris Orogeny, *Geol. Soc. Am. Bull.*, *125*(9-10), 1423–1441, doi:10.1130/B30804.1.

DeLucia, M. S., M. J. Seid, S. Marshak, A. Anders, G. L. Pavlis, X. Yang, H. Gilbert, C. Chen, M. W. Hamburger, and T. Larson (2016), Structural and geomorphological manifestations of the crustal boundary between the Illinois Basin and Ozark Dome: Implications for midcontinent tectonics, paper presented at Geological Society of America Annual Meeting, Geol. Soc. of Am., Denver, Colo., 25–28 Sept.

Domrois, S. L., S. Marshak, C. Abert, and T. H. Larson (2015), ArcGIS maps depicting topography of the basement-cover contact (the Great Unconformity), and the traces of faults and folds, in the Cratonic Platform of the United States, *Search and Discovery Article #30410 (2015)*.

Drahovzal, J. A., D. C. Harris, L. H. Wickstrom, D. Walker, M. T. Baranoski, B. Keith, and L. C. Furer (1992), The East Continent Rift Basin: A new discovery, *Indiana Geol. Surv. Spec. Rep.*, *52*, 25.

Duchek, A. B., J. H. McBride, W. J. Nelson, and H. E. Leetaru (2004), The Cottage Grove fault system (Illinois Basin): Late Paleozoic transpression along a Precambrian crustal boundary, *Geol. Soc. Am. Bull.*, *116*(11), 1465, doi:10.1130/b25413.1.

Ellett, K. M., and S. Naylor (Eds.) (2016), Utility of geological and pedological models in the design of geothermal heat pump systems, *Geol. Soc. Am. Spec. Pap.*, *519*, doi:10.1130/2016.2519(01).

Gorman, A. R., et al. (2002), Deep probe: imaging the roots of western North America, *Can. J. Sci.*, *39*(3), 375–398, doi:10.1139/E01-064.

Hacker, B. R. (1996), Eclogite formation and the rheology, buoyancy, seismicity, and H_2O content of oceanic crust, in *Subduction Top to Bottom*, edited by G. E. Bebout, et al., pp. 337–346, AGU, Washington, D. C., doi:10.1029/GM096p0337.

Hacker, B. R., P. B. Kelemen, and M. D. Behn (2015), Continental lower crust, *Annu. Rev. Earth Planet. Scie.*, *43*, –167, 205, doi:10.1146/annurev-earth-050212-124117.

Harrison, R. W., and A. Schultz (2002), Tectonic framework of the southwestern margin of the Illinois Basin and its influence on neotectonism and seismicity, *Seismol. Res. Lett.*, *73*(5), 698–731.

Hatcher, R. D. (2010), The Appalachian orogen: A brief summary, *Geol. Soc. Am. Mem.*, *206*, 1–19, doi:10.1130/2010.1206(01).

Hauser, E. C. (1996), Midcontinent rifting in a Grenville embrace, in *Basement and Basins of Eastern North America*, edited by B. A. van der Pluijm and P. A. Catacosinos, *Geol. Soc. Am. Spec. Pap., 308*, Boulder, Colo.

Heidlauf, D. T., A. T. Hsui, and G. Klein (1986), Tectonic subsidence analysis of the Illinois Basin, *J. Geol.*, *94*(6), 779–794.

Hickman, J. B. (2011), Structural evolution of an intracratonic rift system; Mississippi Valley Graben, Rough Creek Graben, and Rome Tough of Kentucky, USA, 144 pp., Univ. of Kentucky, Lexington.

Hildenbrand, T. G., and J. D. Hendricks (1995), Geophysical setting of the Reelfoot rift and relations between rift structures and the New Madrid seismic zone, *U.S. Geol. Surv. Prof. Pap., 1538-E*.

Hildenbrand, T. G., A. Griscom, W. R. VanSchmus, and W. D. Stuart (1996), Quantitative investigations of the Missouri gravity low: A possible expression of a large, Late Precambrian batholith intersecting the new Madrid seismic zone, *J. Geophys. Res.*, *101*, 21,921–21,942, doi:10.1029/96JB01908.

Hoffman, P. F. (1988), United plates of America, the birth of a craton—Early Proterozoic assembly and growth of Laurentia, *Ann. Rev. Earth Planet. Sci.*, *16*, 543–603, doi:10.1146/annurev.ea.16.050188.002551.

Kennett, B. L. N., and E. R. Engdahl (1991), Traveltimes for global earthquake location and phase identification, *Geophys. J. Int.*, *105*, 429–465.

Kennett, B. L. N., E. R. Engdahl, and R. Buland (1995), Constraints on seismic velocities in the Earth from travel-times, *Geophys. J. Int.*, *122*(1), 108–124, doi:10.1111/j.1365-246X.1995.tb03540.x.

Klein, G. deV., and A. T. Hsui (1987a), Origin of cratonic basins, *Geology*, *15*, 1094–1098.

Klein, G. deV., and A. T. Hsui (1987b), Origin, evolution, and sedimentary synchroneity of cratonic basins, *AAPG Bull.*, *71*(5), 577–577.

Kolata, D. R., and J. W. Nelson (1997), Role of the Reelfoot Rift/Rough Creek Graben in the evolution of the Illinois Basin, in *Middle Proterozoic to Cambrian Rifting, Central North America*, edited by R. W. Ojakangas, A. B. Dickas and J. C. Green, *Geol. Soc. Am. Spec. Pap., 312*, pp. 287–298, Boulder, Colo.

Langston, C. A. (1994), An integrated study of crustal structure and regional wave propagation for southeastern Missouri, *Bull. Seismol. Soc. Am.*, *84*(1), 105–118.

Langston, C. A. (2011), Wave-field continuation and decomposition for passive seismic imaging under deep unconsolidated sediments, *Bull. Seismol. Soc. Am.*, *101*(5), 2176–2190, doi:10.1785/0120100299.

Lekic, V., S. W. French, and K. M. Fischer (2011), Lithospheric thinning beneath rifted regions of Southern California, *Science*, *334*(6057), 783–787, doi:10.1126/science.1208898.

Liang, C. T., and C. A. Langston (2009), Three-dimensional crustal structure of eastern North America extracted from ambient noise, *J. Geophys. Res.*, *114*, B03310, doi:10.1029/2008JB005919.

Liu, X., and G. L. Pavlis (2013), Appraising the reliability of converted wavefield imaging: Application to USArray imaging of the 410-km discontinuity, *Geophys. J. Int.*, *192*(3), 1240–1254, doi:10.1093/gji/ggs088.

Marshak, S., S. L. Domrois, C. Abert, T. Larson, G. L. Pavlis, M. W. Hamburger, X. Yang, H. Gilbert, and C. Chen (2017), The basement revealed: Tectonic insight from a DEM of the Great Unconformity, USA cratonic platform, *Geology*, doi:10.1130/G38875.1.

Marshak, S., and T. Paulsen (1996), Midcontinent U.S. fault and fold zones: A legacy of Proterozoic intracratonic extensional tectonism?, *Geology*, *24*(2), 151–154.
Marshak, S., and T. Paulsen (1997), Structural style, regional distribution, and seismic implications of Midcontinent fault-and-fold zones, United States, *Seismol. Res. Lett.*, *68*(4), 511–520.
McBride, J. H., and W. J. Nelson (1999), Style and origin of mid-Carboniferous deformation in the Illinois Basin, USA—Ancestral Rockies deformation?, *Tectonophysics*, *305*(1-3), 249–273, doi:10.1016/S0040-1951(99)00015-3.
McBride, J. H., D. R. Kolata, and T. G. Hildenbrand (2003), Geophysical constraints on understanding the origin of the Illinois Basin and its underlying crust, *Tectonophysics*, *363*(1-2), 45–78, doi:10.1016/s0040-1951(02)00653-4.
McBride, J. H., H. E. Leetaru, R. A. Bauer, B. E. Tingey, and S. E. A. Schmidt (2007), Deep faulting and structural reactivation beneath the southern Illinois Basin, *Precambrian Res.*, *157*(1-4), 289–313, doi:10.1016/j.precamres.2007.02.020.
McGlannan, A. J., and H. Gilbert (2016), Crustal signatures of the tectonic development of the North American Midcontinent, *Earth Planet. Sci. Lett.*, *433*, 339–349, doi:10.1016/j.epsl.2015.10.048.
Mooney, W. D., M. C. Andrews, A. Ginzburg, D. A. Peters, and R. M. Hamilton (1983), Crustal structure of the Northern Mississippi Embayment and a comparison with other continental rift zones, *Tectonophysics*, *94*(1-4), 327–348, doi:10.1016/0040-1951(83)90023-9.
Nelson, K. D., and J. Zhang (1991), A COCORP deep reflection profile across the buried Reelfoot Rift, South-Central United-States, *Tectonophysics*, *197*(2-4), 271–293, doi:10.1016/0040-1951(91)90046-U.
Nelson, W. J. (1995), Structural features in Illinois, *Illinois State Geol. Surv. Bull.*, *100*, 144.
Nelson, W. J., and D. K. Lumm (1985), Ste. Genevieve Fault Zone, Missouri and Illinois, *Illinois Geol. Sur. Contract Grant Rep.*, *1985*(3), 1–92.
Nelson, W. J., D. K. Lumm, and Illinois State Geological Survey, and Geological Society of America (1992), Structure and tectonics of the Rough Creek Graben: Western Kentucky and Southeastern Illinois, 30 pp., Dep. of Energy and Natural Resources, Champaign, Ill.
Nelson, W. J., and S. Marshak (1996), Devonian tectonism of the Illinois basin region, U.S. continental interior, in *Basement and Basins of Eastern North America*, edited by B. A. van der Pluijm and P. A. Catacosinos, *Geol. Soc. Am. Spec. Pap.*, pp. 169–179, Boulder, Colo.
Noger, M. C., and J. A. Drahovzal (2005), Lithostratigraphy of precambrian and paleozoic rocks along structural cross section Ky-1, Crittenden County to Lincoln County, Kentucky, in *Report of Investigations*, pp. 1–29, Kentucky Geol. Surv., Univ. of Kentucky, Lexington.
Okure, M. S., and J. H. McBride (2006), Deep seismic reflectivity beneath an intracratonic basin: Insights into the behavior of the uppermost mantle beneath the Illinois Basin, *Precambrian Res.*, *149*(3-4), 99–125, doi:10.1016/j.precamres.2006.04.006.
Parker, E. H., R. B. Hawman, K. M. Fischer, and L. S. Wagner (2013), Crustal evolution across the southern Appalachians: Initial results from the SESAME broadband array, *Geophys. Res. Lett.*, *40*, 3853–3857, doi:10.1002/grl.50761.
Parker, E. H., R. B. Hawman, K. M. Fischer, and L. S. Wagner (2015), Constraining lithologic variability along the Alleghanian detachment in the southern Appalachians using passive-source seismology, *Geology*, *43*(5), 431–434, doi:10.1130/G36517.1.
Pavlis, G. L. (2011a), Three-dimensional wavefield imaging of data from the USArray: New constraints on the geometry of the Farallon slab, *Geosphere*, *7*(3), 785–801, doi:10.1130/Ges00590.1.
Pavlis, G. L. (2011b), Three-dimensional, wavefield imaging of broadband seismic array data, *Comput. Geosci.*, *37*(8), 1054–1066, doi:10.1016/j.cageo.2010.11.015.
Pavlis, G. L., and Y. Wang (2015), Shaping wavelet effects in scattered wave imaging of *P* to *S* conversion data, *Geophys. J. Int.*, *203*(1), 373–383, doi:10.1093/gji/ggv163.
Pavlis, G. L., A. J. Rudman, B. M. Pope, M. W. Hamburger, G. W. Bear, and H. Al-Shukri (2002), Seismicity of the Wabash Valley seismic zone based on a temporary seismic array experiment, *Seismol. Res. Lett.*, *73*(5), 751–761.
Pollitz, F. F., and W. D. Mooney (2016), Seismic velocity structure of the crust and shallow mantle of the Central and Eastern United States by seismic surface wave imaging, *Geophys. Res. Lett.*, *43*, 118–126, doi:10.1002/2015GL066637.
Poppeliers, C., and G. L. Pavlis (2003), Three-dimensional, prestack, plane wave migration of teleseismic *P*-to-*S* converted phases: 1. Theory, *J. Geophys. Res.*, *108*(B2), 2112, doi:10.1029/2001JB000216.
Pratt, T. L., R. Culotta, E. C. Hauser, D. Nelson, L. Brown, S. Kaufman, J. Oliver, and W. Hinze (1989), Major Proterozoic basement features of the eastern midcontinent of North America revealed by recent COCORP profiling, *Geology*, *17*, 505–509.
Pratt, T. L., E. C. Hauser, and K. D. Nelson (1992), Widespread buried Pracambrian layered sequences in the U.S. Mid-continent: Evidence for large Proterozoic depositional basins, *AAPG Bull.*, *76*(9), 1384–1401.
René, R. M., and F. L. Stanonis (1995), Reflection seismic profiling of the Wabash Valley Fault System in the Illinois Basin, *U.S. Geol. Surv. Prof. Pap.*, *1538-O*.
Ringwood, A. E., and D. H. Green (1966), An experimental investigation of the gabbro-eclogite transformation and some geophysical implications, *Tectonophysics*, *3*(5), 383–427, doi:10.1016/0040-1951(66)90009-6.
Rumpfhuber, E. M., G. R. Keller, E. Sandvol, A. A. Velasco, and D. C. Wilson (2009), Rocky Mountain evolution: Tying continental dynamics of the Rocky Mountains and Deep Probe seismic experiments with receiver functions, *J. Geophys. Res.*, *114*, B08301, doi:10.1029/2008JB005726.
Savage, B., B. M. Covellone, and Y. Shen (2017), Wave speed structure of the eastern North American margin, *Earth Planet. Sci. Lett.*, *459*, 394–405, doi:10.1016/j.epsl.2016.11.028.
Schulte-Pelkum, V., and K. H. Mahan (2014), A method for mapping crustal deformation and anisotropy with receiver functions and first results from USArray, *Earth Planet. Sci. Lett.*, *402*, 221–233, doi:10.1016/j.epsl.2014.01.050.
Shen, W. S., and M. H. Ritzwoller (2016), Crustal and uppermost mantle structure beneath the United States, *J. Geophys. Res. Solar Earth.*, *121*, 4306–4342, doi:10.1002/2016JB012887.
Stein, S., and M. Liu (2009), Long aftershock sequences within continents and implications for earthquake hazard assessment, *Nature*, *462*(7269), 87–89, doi:10.1038/nature08502.
Stein, S., et al. (2016), New insights into North America's Midcontinent Rift, *Eos*, 10–16, doi:10.1029/2016EO056659.
Tao, K., T. Liu, J. Ning, and F. Niu (2014), Estimating sedimentary and crustal structure using wavefield continuation: Theory, techniques and applications, *Geophys. J. Int.*, *197*(1), 443–457, doi:10.1093/gji/ggt515.
Thybo, H., and I. M. Artemieva (2013), Moho and magmatic underplating in continental lithosphere, *Tectonophysics*, *609*, 605–619, doi:10.1016/j.tecto.2013.05.032.
Wang, Y., and G. Pavlis (2016), Generalized iterative deconvolution for receiver function estimation, *Geophys. J. Int.*, *204*(2), 1086–1099, doi:10.1093/gji/ggv503.
Ward, K. M., R. C. Porter, G. Zandt, S. L. Beck, L. S. Wagner, E. Minaya, and H. Tavera (2013), Ambient noise tomography across the central Andes, *Geophys. J. Int.*, *194*(3), 1559–1573, doi:10.1093/gji/ggt166.
Wheeler, R. (1997), Boundary separating the seismically active reelfoot rift from the sparsely seismic Rough Creek Graben, Kentucky and Illinois, *Seismol. Res. Lett.*, *68*(4), 586–598.

Whitmeyer, S. J., and K. E. Karlstrom (2007), Tectonic model for the Proterozoic growth of North America, *Geosphere*, *3*(4), 220–259, doi:10.1130/Ges00055.1.

Wright, C., M. T. O. Kwadiba, R. E. Simon, E. M. Kgaswane, and T. K. Nguuri (2004), Variations in the thickness of the crust of the Kaapvaal craton, and mantle structure below southern Africa, *Earth Planets Space*, *56*(2), 125–137.

Yang, X. (2016), Seismic imaging of the lithosphere beneath the southern Illinois Basin and its tectonic implications, 231 pp., Indiana Univ., Bloomington.

Yang, X. T., G. L. Pavlis, M. W. Hamburger, E. Sherrill, H. Gilbert, S. Marshak, J. Rupp, and T. H. Larson (2014), Seismicity of the Ste. Genevieve Seismic Zone based on observations from the EarthScope OIINK Flexible Array, *Seismol. Res. Lett.*, *85*(6), 1285–1294, doi:10.1785/0220140079.

Yang, X. T., G. L. Pavlis, and Y. Wang (2016), A quality control method for teleseismic *P*-wave receiver functions, *Bull. Seismol. Soc. Am.*, *106*(5), 1948–1962, doi:10.1785/0120150347.

Yu, C. Q., W. P. Chen, J. Y. Ning, K. Tao, T. L. Tseng, X. D. Fang, Y. J. Chen, and R. D. van der Hilst (2012), Thick crust beneath the Ordos plateau: Implications for instability of the North China craton, *Earth Planet. Sci. Lett.*, *357*, 366–375, doi:10.1016/j.epsl.2012.09.027.

Yu, Y. Q., J. G. Song, K. H. Liu, and S. S. Gao (2015), Determining crustal structure beneath seismic stations overlying a low-velocity sedimentary layer using receiver functions, *J. Geophys. Res. Solar Earth*, *120*, 3208–3218, doi:10.1002/2014JB011610.

Zhao, W. J., and K. D. Nelson (1993), Deep seismic-reflection evidence for continental underthrusting beneath southern Tibet, *Nature*, *366*(6455), 557–559, doi:10.1038/366557a0.

Zheng, T. Y., Y. M. He, J. H. Yang, and L. Zhao (2015), Seismological constraints on the crustal structures generated by continental rejuvenation in northeastern China, *Sci. Rep.*, *5*, doi:10.1038/srep14995.